Proton-Coupled Electron Transfer in DNA on Formation of Radiation-Produced Ion Radicals

Anil Kumar and Michael D. Sevilla*

Department of Chemistry, Oakland University, Rochester, Michigan 48309

Received January 25, 2010

Contents

* To whom correspondence should be addressed. E-mail: sevilla@oakland.edu.

1. Introduction

It is well established that exposure of DNA to high-energy radiation results in a variety of physical and chemical changes in DNA including strand breakage, mutation, and DNA damage.[1−16] Initially, high-energy radiation randomly ionizes or excites DNA components (base, sugar, and phosphate backbone) as well as the surrounding water molecules, which are an integral part of the DNA structure. Holes produced quickly shed excess energy and result in ground-state cation radicals.[12−15,17,18] Secondary electrons with kinetic energy are produced in a large quantity (4×10^4 per MeV of energy deposited)[19] along the tracks of the ionizing radiation and have been recently shown to produce single- and double-strand breaks in DNA.[20−26] Only a small fraction of the secondary electrons are able to cause DNA damage. Most secondary electrons undergo collisional loss of energy with the medium and thermalize within picoseconds. They then either recombine with holes or are captured by the pyrimidines (thymine (T) and cytosine (C)) to form DNA radical anions $T^{\bullet-}$ and $C^{\bullet-}$.[27] Holes produced during the initial ionizing event in DNA for the most part transfer to the base with the lowest ionization potential. Guanine (G) has the lowest ionization potentials of the four DNA bases (adenine (A), T, G, and C),[28−31] and as a consequence, guanine becomes the locus for hole trapping in DNA.[32−34] Ionization of the sugar phosphate backbone initiates two competitive reactions for the hole formed: (i) deprotonation from sugar ring carbon sites to form neutral sugar radicals[34−39] and (ii) hole transfer to a neighboring DNA base that after *base-to-base* hole transfer would end up on guanine.[37,38,39b] Figure 1 gives an overview of the processes that lead from radiation-induced hole and secondary electron generation in DNA to hole and electron transfer, proton transfer processes, and subsequent molecular product formation such as 8-oxo-G from $G^{\bullet+}$.[32−34] Proton-coupled electron and hole transfer is an important feature of the radiation damage process. An example is the equilibrium shown in Figure 1, left side, in which protonation of the cytosine anion radical at N_3 results in transfer of electrons from thymine to cytosine. Coupling of these prototropic equilibria to charge transfer of radiation-produced ion radicals is the focus of this review.

One-electron oxidation or reduction of a molecule profoundly affects the acid/base properties of the molecule. On loss of one electron, DNA bases greatly increase in acidity, whereas, on gain of one electron, DNA bases become substantially more basic in comparison to the neutral base.

10.1021/cr100023g
Published on Web 05/05/2010

Michael D. Sevilla is currently Distinguished Professor of Chemistry at Oakland University. He received a B.S. in chemistry from San Jose State College and a Ph.D. in physical chemistry from the University of Washington in 1967. After a postdoctoral year at the University of Washington and two years with Atomics International Corp., he joined Oakland University in 1970. He has been Chair of the Chemistry Department at Oakland University, 1997−2003, Associate Editor of *Radiation Research*, 2003−2006, and President of the Radiation Research Society, 2005−2006. Professor Sevilla is a well-known radiation chemist and has focused his research on free radical reactions induced by radiation damage to DNA and other biomolecules employing experimental approaches such as electron spin resonance spectroscopy and theoretical approaches such as density functional theory. Recent efforts in collaboration with Dr. Kumar have elucidated the role of excited states of DNA ion radicals in the formation of DNA damage. He is a member of the AAAS, the ACS, and the Radiation Research Society.

Anil Kumar received his Ph.D. in physics from the Department of Physics, Banaras Hindu University, Varanasi, India. His Ph.D. dissertation investigated the structure, properties, and specific molecular interactions of DNA and its constituents using quantum chemical methods. He was awarded a position as Pool Scientist from the Council of Scientific and Industrial Research (CSIR), New Delhi, India, in 1997. Later he did his postdoctoral work at the Department of Chemistry, University of Hannover, Germany. He was a visiting scientist at the Department of Molecular Biophysics, German Cancer Research Institute, DKFZ, Heidelberg, Germany. Presently, he is working as a research associate in the group of Prof. M. D. Sevilla at the Department of Chemistry, Oakland University. His research interests are to explore the mechanism of DNA damage, DNA ion radical formation, the charge transfer process, and the involvement of excited states for producing DNA strand breaks employing computational chemistry approaches.

Steenken[40−42] considered the proton transfer reactions in base pair ion radicals where hydrogen-bonded protons likely transfer between the base pairs. In his pioneering work, he showed that the acidity of the one-electron-oxidized purine base and the basicity of the one-electron-reduced pyrimidine base would affect the extent of such inter base pair proton transfer reactions. Proton coupling with the hole or electron transfer processes in DNA plays a vital role in controlling the charge transfer process in DNA.[40] It is well-known that proton-coupled electron transfer (PCET) or proton-coupled hole transfer (PCHT) reactions are crucial for biological processes such as photosynthesis,[43−48] respiration,[49,50] and enzyme reactions[51] and in oxidized DNA duplexes.[52,53] From the early 1990s to the present, several reviews considering the experimental aspects of PCET from the groups of Shafirovich,[52] Meyer,[54,55] Thorp,[53,55−57] Mayer,[58,59] Babcock,[60] Stubbe,[61] Robert,[62] and Costentin[63] and their co-workers have appeared in the literature while a series of excellent theoretical reviews on PCET have become available from the groups of Cukier,[64] Hammes-Schiffer,[65−70] and Nocera.[64,71] Application of quantum chemical methods to explore the redox enzymes including PCET have also appeared.[72,73]

While PCET is critical to charge transfer in DNA, only a few reviews have covered PCET aspects of the charge transfer process in DNA.[61−63] In this review we first treat hole and electron transfer processes in DNA which lead to ion radical localization in DNA. A brief description of theoretical treatments of PCET is then presented. Finally, in the present review we report on experimental and theoretical examples from the work of a number of groups, including our own, which illustrate the role of PCET in long-range hole/electron transfer in DNA, formation of oxidized and reduced DNA bases and base pairs in ground and excited states, and resulting sugar radical formation.

2. Background of Charge Transfer in DNA

The hypothesis that π-orbital overlap of paired bases in DNA can serve as a pathway for charge migration in DNA was proposed in 1962 by Eley, Spivey, and Leslie[74,75] from conductivity measurements of DNA[75] and its bases (A, T, G, and C).[74] This led to suggestions that DNA could be a conductor,[76] a semiconductor,[77] or even an insulator.[78,79] Since then, an enormous interest in DNA-mediated charge transfer has grown in order to understand its role in biological cellular process[80,81] and its use in DNA-based electrochemical devices,[82−86] which have broadened our views of the complex nature of DNA charge transfer.

While the generation of hole and excess electron sites in DNA can be accomplished by physical means such as γ-irradiation or photoexcitation, chemically induced one-electron oxidation or reduction, also, may lead to holes and excess electron sites in DNA. After formation of holes or excess electrons, charge transfer through DNA ensues to more thermodynamically favorable sites. Thus, DNA-mediated charge transfer can employ either oxidative hole transfer or reductive electron transfer processes. In fact, hole transfer is always accompanied by the transfer of an electron in the opposite direction. Therefore, hole transfer and electron transfer are both electron transfer reactions; see Figure 2. However, for the purposes of this review, hole transfer is employed to describe transfers originating from an electron loss center whereas electron transfer refers to those processes begun by addition of an excess electron to the system. Hole transfer chiefly migrates through the highest occupied molecular orbital (HOMO) of the system, whereas electron transfer migrates through the lowest unoccupied molecular orbital (LUMO). Despite its obvious biological and technological significance, the mechanism of long-distance hole migration in DNA resulting from oxidative damage has been controversial and continues to be an exciting area of research.[87−89]

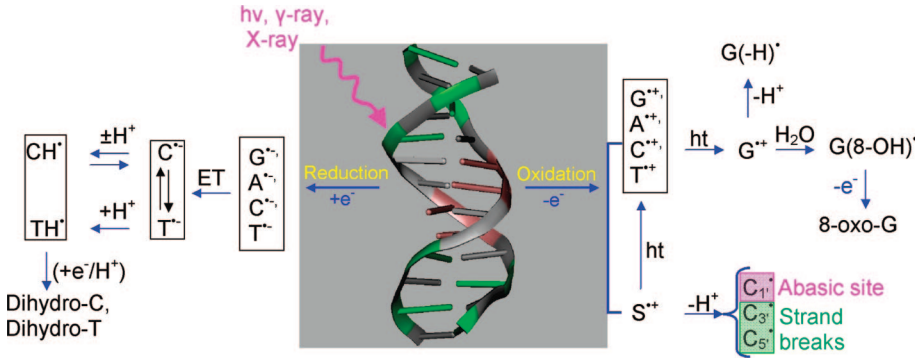

Figure 1. Schematic diagram showing major oxidation and reduction processes that occur in DNA during high-energy radiation interaction with DNA (ht = hole transfer; ET = electron transfer). Processes involving excited states and low-energy electrons are not shown. The sketch is based on the work from refs 3, 7, 9−17, and 31−42.

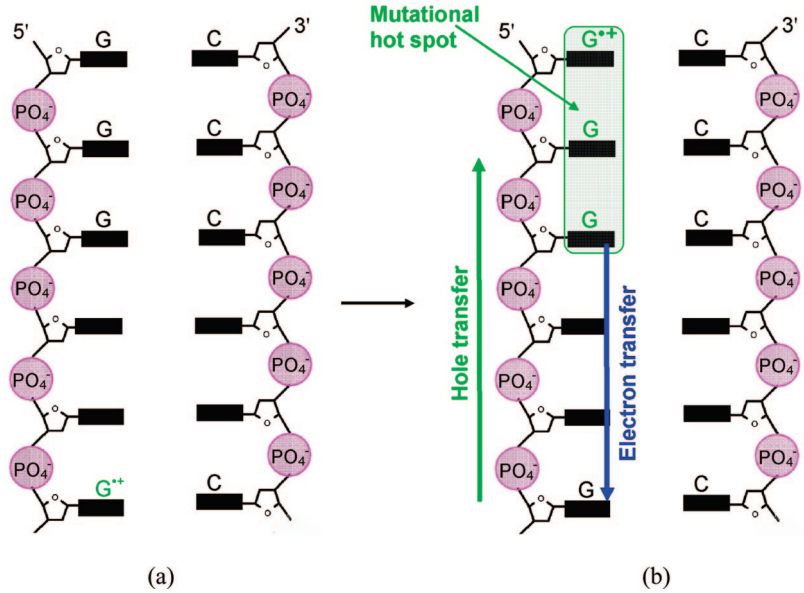

Figure 2. (a) One-electron oxidation of G in DNA is followed by (b) hole transfer to a distant GGG (mutational hot spot). This figure is based in part on ref 101. Hole localization is mainly at the 5′-G on the basis of electron spin resonance measurements from ref 119.

2.1. Oxidatively Induced Hole Transfer

In the late 1990s a number of experiments[76,90−93] demonstrated that one-electron-oxidized guanine, generated by selective oxidation of DNA, could induce a hole migration to a distant guanine through the stacked base pairs of DNA; in these experiments oxidation (charge injection) of DNA was induced by photoexcitation. In the photoexcitation process, an electron is transferred from DNA to the photoexcited chromaphore, injecting a hole into DNA which transfers from the charge donor to the final acceptor. Barton and co-workers[76,90,91,95−98] inserted donor- and acceptor-type intercalators into DNA oligomers to investigate charge transfer within DNA. In their experiments the efficiency of the charge transfer depends on several factors, such as (i) coupling of the redox probes (intercalators) to the π-stacked base pairs, (ii) coupling between the bases in duplex DNA, (iii) the presence of base-pair mismatch in the intervening DNA bridge, and (iv) DNA dynamics. Giese and co-workers[99−102] used another approach for charge injection into DNA which is achieved by the photolytic generation of a $C_{4'}$ sugar radical via Norrish type I photocleavage from 4′-*tert*-butyl ketones at specific sites in deoxynucleotides which rearrange to an enol−ether radical cation via β-phosphate elimination, resulting in a strand break. The enol ether radical cation subsequently oxidizes a nearby guanine in the DNA duplex.[99,103] A competition exists between hole transfer and water addition to $G^{\bullet+}$, the latter of which results in further oxidation in 8-oxo-G and other oxidatively modified guanines.[32,34,104,105] These products allow for selective DNA strand cleavage by base or enzymatic treatment and are detected by gel electrophoresis.[99] In this approach, the relative charge transfer rate in DNA may be obtained by measuring the product yield of oxidatively modified guanine as a function of the distance between guanines and the site of the enol ether radical cation. Lewis[106−109] used covalently attached stilbene in DNA hairpins along with time-resolved spectroscopy to follow the charge transfer process. Schuster[110−112] employed anthraquinones attached to the DNA strand. Photoexcitation of anthraquinone covalently attached with DNA oxidizes a guanine to form the anthraquinone radical anion and $G^{\bullet+}$ in an overall triplet state.[110] Hole transfer was monitored by 8-oxo-G formation. Some one-electron oxidants used in the above experiments are shown in Figure 3.

The hole generated in DNA on a single G (see Figure 2a), by any one of the techniques described above, transfers to sites having GG or GGG sequences in DNA (see Figure 2b) because of their lower oxidation potential compared to that of a single G.[113−118] On the basis of theoretical calculations,[113−115] Ratner and co-workers[118] proposed the ionization potential (IP) of GG and GGG to be lower than that of G by 0.5 and

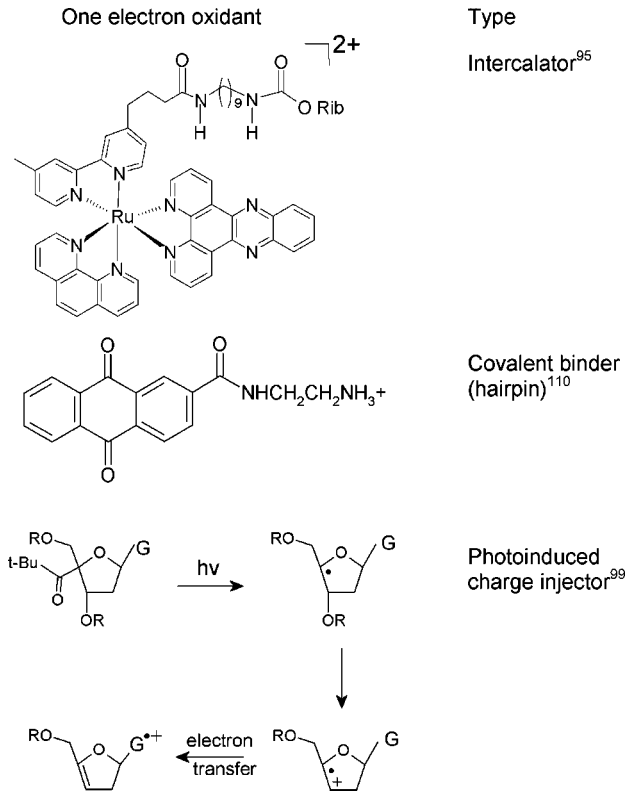

Figure 3. Structures of one-electron oxidants (a, top) tethered ruthenium II derivative[95] and (b, middle) anthraquinone derivative[110] and (c, bottom) one-electron oxidation of G by photolysis of *tert*-butyl ketone attached to the $C_{4'}$ site of sugar.[99]

0.7 eV, respectively, concluding that GG and GGG are deeper hole-trapping sites. However, using experiment and theory, Lewis[116] and Conwell[117] reported much smaller hole-trapping energies ranging from 0.051 to 0.081 eV, respectively. In the sequences 5′-GG-3′ and 5′-GGG-3′, the 5′-site was observed to be the preferred site for oxidative damage followed by a small contribution from neighboring guanines.[90,113,114,119] These one-electron-oxidized [GG] or [GGG] sequences in DNA serve as the mutational hot spot and can be detected biochemically and used as a marker of hole transfer.

2.2. Reductive Electron Transfer

An excess electron added to the DNA from a photoexcited donor or γ-irradiated DNA samples can migrate within DNA to the final electron acceptor, and this process is known as reductive electron transfer or electron transfer. In contrast to hole transfer, which is mediated via the DNA bases with the lowest oxidation potentials, i.e., the purines, electron transfer is guided by pyrimidines, which have the lowest reduction potentials and highest electron affinities of the DNA bases. Compared to hole transfer, there is significantly less knowledge about processes involved in excess electron transfer within DNA. Electron transfer rates in DNA from base radical anions to electron acceptor intercalators have been studied using pulse radiolysis experiments.[120,121] Also, Sevilla and co-workers[122,123] used electron spin resonance (ESR) spectroscopy to investigate electron transfer in DNA using electron acceptor intercalators such as mitoxantrone, ethidium bromide, and phenanthroline dissolved in LiBr aqueous glassy medium at low temperatures. The samples were γ-irradiated to produce excess electrons which added to DNA. Subsequent electron transfer from DNA base anion radicals to randomly placed intercalators within DNA was detected by the loss of the DNA radical anion ESR signal and the buildup of the intercalator electron adduct signal with time at 77 K.

Electron injections in DNA have also been carried out using photochemical methods. Carell and co-workers[124,125] used flavin derivatives and incorporated them into oligonucleotides for electron injection into DNA. Lewis et al.[126] used stilbene diether derivatives as DNA hairpins which upon excitation transfer an excess electron to the pyrimidines in DNA. Giese et al.[127] employed a 5-substituted thymidine which when inserted into DNA double-stranded oligomers and photoexcited formed a substituted thymine radical anion via a Norrish I type reaction. This injects an electron into the DNA duplex and causes thymine dimer cleavage at long distances. Pyrene-modified pyridine nucleosides were used by Wagenknecht et al.[94] One-electron reductants used to inject an electron into the DNA are shown in Figure 4.

2.3. Mechanism of Charge Transport (Superexchange vs Hopping)

The distance-dependent charge transfer rate k_{CT} can be simply expressed by[128−130]

$$\text{for tunneling: } k_{CT} = k_0 e^{-\beta \Delta r} \quad (1a)$$

$$\text{for hopping: } k_{CT} = k_{ih}/N^{\eta} \ (\eta = 2) \quad (1b)$$

In eq 1a, k_{CT} is the charge transfer rate, Δr is the distance between the donor and acceptor, and β is related to the height of the barrier through which the charge tunnels. In eq 1b, N is the number of hopping steps and k_{ih} is the rate for interbase charge transfer. Both processes are active at ambient temperatures, and these equations are thus simplifications. More theoretically satisfying treatments have been presented in

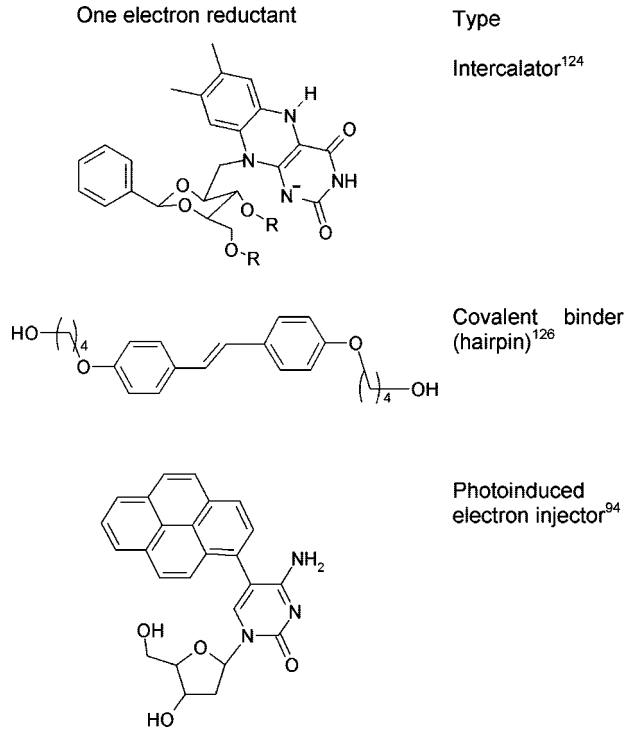

Figure 4. Structures of one-electron reductants (a, top) riboflavin coenzyme nucleobase,[124] (b, middle) stilbene diether (SE) linkers,[126a] and (c, bottom) pyrene-modified nucleosides.[94]

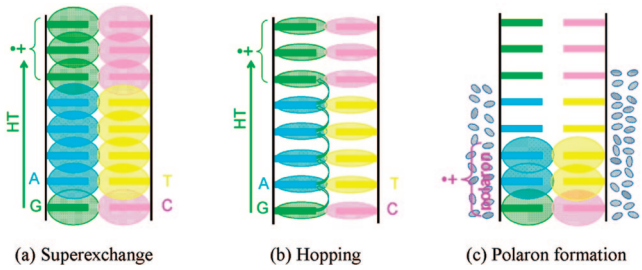

Figure 5. Proposed DNA-mediated charge transfer mechanisms: (a) superexchange (the overlapping MOs on the well-stacked DNA bases provide a path for fast hole transfer), (b) hopping (the MOs are localized on the DNA bases, and the hole hops from one base to another, shown by arrows), (c) polaron formation occurs as the solvent polarizes around DNA holes. This limits hole delocalization and transfer rates.

which these processes are not separated.[131] However, these two extremes provide a convenient way of visualizing the ongoing processes. For tunneling, exponential falloff with distance is expected to limit charge transfer to only a few base pairs unless β is quite low. Thus, when experiments demonstrated long-range (ca. 200 Å) hole migration in DNA, Barton et al.[76,90,132−134] proposed DNA as a molecular wire having delocalized molecular orbitals (MOs) on the stacked DNA bases (see Figure 5a) and reported a fast charge transfer rate of ca. 10^{-10} s^{-1} with an appreciably small β value of 0.1 $Å^{-1}$. The apparent small β value has been confirmed in other charge transfer experiments using similar systems, but alternative interpretations have been proposed for the charge transfer reactions in DNA. The photoinduced electron transfer studies proposed the multistep hopping model[101,108,110,112,118,128] where the hole hops from one base to the adjacent base as shown in Figure 5b. This mechanism follows a diffusional rate process which falls off much more slowly than the tunneling mechanism, giving the low apparent β value. If the hole hops through intervening guanines, the process is known as "G-hopping" and if adenines are the charge carrier, the process is known as "A-hopping". The situation is different when two guanines are separated by several adenines. Giese and co-workers[135] demonstrated experimentally that if two guanines are separated by several adenines, the rate of charge transfer decreases rapidly for short distances (≤13.6 Å), showing a typical tunneling distance dependence; however, for large distances (>13.6 Å) the rate of charge transfer is only weakly distance dependent as expected for a diffusional (hopping) process. This important result shows that for short distances charge transfers through tunneling (superexchange) while long-range charge transfer is mediated by thermally induced hopping between adenine bases (A-hopping).[135] Thus, tunneling components would have β values between 0.6 and 1.2, whereas, when hopping is operative, these values would appear far lower. For example, Giese and co-workers[93,101,136] reported β values of 0.7 ± 0.1 and 1.0 $Å^{-1}$. Lewis and co-workers[108,137] observed the β values for DNA-capped stilbenes in their excited state (ES) and ground state (GS) as 0.7 ± 0.1 $Å^{-1}$ (ES), 0.63 ± 0.1 $Å^{-1}$ (ES), and 0.61 ± 0.1 $Å^{-1}$ (GS). Fukui and Tanakat[138] reported the β value 1.42 $Å^{-1}$ for the intercalated acridine−DNA system in the excited state. The theoretically calculated $\beta \approx 1.2-1.6$ $Å^{-1}$ from the work of Priyadarshy et al.[77,78] are higher than experimental β values. Siebbeles and co-workers[139] also calculated the β values for a donor and acceptor separated by several AT bridges using the tight-binding approach and Miller−Abrahams model of incoherent hopping. The calculated β value varies with the height of the barrier and ranges from 0.1 to 1.0 $Å^{-1}$.

Using density functional theory (DFT) and Hartree−Fock (HF) methods, Olofsson and Larsson[140] also calculated β values for several sequences in the range 0.68−1.68 $Å^{-1}$, which is in good agreement with experiment. Thus, results to date clearly show holes and electrons travel through DNA by a combination of tunneling and hopping mechanisms, which might classify DNA as a semiconductor but a semiconductor whose properties can be easily manipulated by the base composition. Indeed, this classification is too simplistic, and more complexities must be taken into account such as polaron formation[141−144] and structural and solvent dynamics.[145,146] Charge injection into a molecule causes the surrounding environment (water) to polarize by partially delocalizing the charge on adjacent bases (see Figure 5c) and lowering the energy of the system.[141] Using theoretical calculations, Conwell has shown that polaron formation may be delocalized over 2−5 base pairs, depending on the sequence.[142−144] A few reviews[147−150] covering this topic in detail have appeared in the literature.

Here we simply emphasize radical generation in DNA which can occur from one-electron oxidative and reductive pathways as shown in Figure 1. Once these ion radicals are formed, they migrate within the DNA to the most stable trapping sites. It is also known that one-electron oxidation or reduction of a nucleobase changes the pK_a drastically and DNA bases become substantially more acidic on oxidation and more basic on reduction. Protonation/deprotonation reactions then take place either within the hydrogen-bonded base pair or from the surrounding medium, i.e., hydration shell. As a result, hole and excess electron transfer most often become coupled to proton transfers and limit the charge transfer process in DNA. The occurrence of such PCET or PCHT in DNA also depends on the rate of charge transfer vs the rate of proton transfer. In such situations, proton transfer must be fast (ps)[40] to compete with the hole and electron transfer rate, which lies in the range 10^8-10^{12} s^{-1}.[137] Such PCET or PCHT is the focus of our review and will be discussed in sections 4 and 5.

3. Proton-Coupled Electron Transfer (Conceptual Background)

PCET reactions are important pathways in mediating a variety of processes in biology and chemistry.[43−53] In contrast to simple electron transfer (ET) or proton (H^+) transfer (PT) reactions, PCET is more complex as both an electron and a proton must transfer and their coupling strongly influences the process thermodynamically and kinetically. In PCET, the transfer of an electron and a proton may be sequential (stepwise) or concerted.[54,64] In sequential transfer, either the electron or proton transfers first, and this is termed sequential PCET or ET−PT or PT−ET. In the concerted mechanism, the electron and proton transfer simultaneously, and this is termed CPET.[54,64] Since electrons and protons both behave quantum mechanically with wave and particle nature, these two processes (sequential and concerted) can be difficult to distinguish from one another.[54,55,61,64,66,151] Hydrogen atom transfer (HAT) involves a concerted process in which an electron and a proton transfer as a nearly single neutral entity.[66] Finally, hydride (H^-) transfer can also be considered a PCET as it involves two electrons and a proton transfer.[66]

The schematic diagram for sequential and concerted pathways for PCET is shown in Figure 6. In Figure 6, the

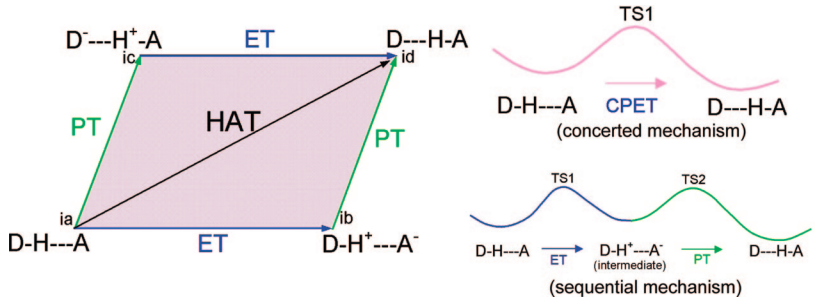

Figure 6. Schematic diagram showing stepwise (sequential) electron transfer and proton transfer (ET−PT or PT−ET) processes which proceed along the sides of the parallelogram. In ET−PT the reaction path has two transition states, TS1 and TS2, lower right. The entire area of the parallelogram represents the PCET mechanism, and the reaction has only one transition state (TS1), upper right. D−H is the electron and proton donor, and A is the acceptor. This figure is based on refs 61, 151, and 164.

arrows at the edges of the parallelogram show the direction of electron (blue color) and proton (green color) transfer while the four corners (ia, ib, ic, and id) of the parallelogram correspond to possible states of the system starting with (ia) a proton and electron donor (D−H) hydrogen bonded to the acceptor A (D−H···A). The processes then follow as proton donation to ic followed by electron transfer to id or electron transfer to ib followed by proton transfer to id. In this representation, arrows, shown at the edges of the parallelogram, correspond to the sequential transfer of the electron and proton (ET−PT or PT−ET). The diagonal arrow shows the concerted electron and proton transfer (CPET) or HAT, and PCET includes the entire area of the parallelogram,[151,152] shown in purple. In CPET, the reaction involves only one transition state (TS1) and no intermediate states are formed (see Figure 6) but electron and proton events can be asynchronous or synchronous. In the sequential mechanism, two transition states (TS1 and TS2), joined by an intermediate, are formed, as shown in Figure 6. Since, in this case, electron and proton transfer events are separated, the overall reaction rate constant (k) is given by

$$k^{-1} = k_{ET}^{-1} + k_{PT}^{-1} \quad (2)$$

where k_{ET} and k_{PT} are electron and proton transfer rate constants, respectively.[151,152] From Figure 6, it is evident that PCET (inside the parallelogram) and stepwise (edge) mechanisms are difficult to distinguish from each other, if PCET is kinetically fast. To aid the investigations of PCET reactions, a number of theoretical methods have been developed by Cukier[152−157] and Hammes-Schiffer[158−163] and their co-workers as well as by others.[164−166] The rate constant expression for a fixed proton donor and acceptor distance R for nonadiabatic PCET reactions in solution is given by[159]

$$k = \sum_{\mu} P_{\mu} \sum_{\nu} \frac{|V^{el} S_{\mu\nu}^{(0)}|^2}{\hbar} \sqrt{\frac{\pi}{\lambda_{\mu\nu} K_B T}} \exp\left[-\frac{(\Delta G_{\mu\nu}^0 + \lambda_{\mu\nu})^2}{4\lambda_{\mu\nu} K_B T}\right] \quad (3)$$

In eq 3, P_μ is the Boltzmann probability for the reactant state μ, V^{el} is the electronic coupling, $S_{\mu\nu}^{(0)}$ is the proton vibrational wave function overlap, $\Delta G_{\mu\nu}^0$ is the free energy of reaction for vibronic states μ and ν, $\lambda_{\mu\nu}$ is the total reorganizational energy, K_B is the Boltzmann constant, and T is the temperature. The term $V^{el}S_{\mu\nu}^{(0)}$ in eq 3 gives the mixing of electronic coupling with vibrational wave function overlap of the proton in its initial and final states. The square of $S_{\mu\nu}^{(0)}$ gives the measure of the extent to which the reactant and product coexist along the proton transfer coordinate. Generally, the

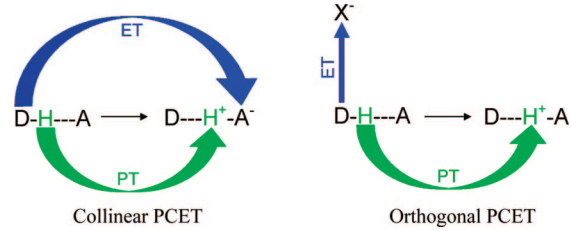

Figure 7. Collinear and orthogonal PCET. In collinear PCET, the proton and electron transfer to the same acceptor site (A). In orthogonal or bidirectional PCET, the proton and electron transfer to two different acceptor sites, X (electron acceptor) and A (proton acceptor).

vibrational overlap $S_{\mu\nu}^{(0)}$ of the proton is small because the proton mass is about 1840 times the mass of the electron. From the de Broglie wavelength $\lambda = h/(2mE)^{1/2}$ the wavelength of a proton is about 40 times smaller than that of an electron for a fixed energy. Thus, the proton's vibrational wave function decreases more rapidly with distance in comparison to electronic wave functions. A small change in proton transfer distance can therefore greatly affect the vibrational overlap $S_{\mu\nu}^{(0)}$ and the overall PCET reaction.

From experiments it is also found that the electron and proton can transfer to different acceptor sites and fall into the category of PCET.[54,55,151] Depending on the nature and location of the electron and proton acceptor sites, PCET can be classified as (i) collinear and (ii) orthogonal. In collinear PCET, the electron and proton transfer to the same acceptor site, while, in orthogonal PCET, the electron and the proton transfer to different acceptor sites as shown in Figure 7. The orthogonal PCET is also termed as bidirectional or multisite electron and proton transfer (MSEPT).[54] From theoretical calculations, it is also found that proton motion can affect the electron transfer even though they do not transfer to the same acceptor site (orthogonal PCET). Also, in certain circumstances the same electron and proton need not be coupled during their entire transformation. During transfer the electron may actually encounter different protons in a transport chain. Therefore, kinetic and thermodynamic measurements provide evidence for any coupling between a moving electron and a specific proton or a set of protons at any given time. It is also emphasized that any motion of the coupled proton from its initial position affects the PCET kinetics. Thus, the complete transfer of the proton is not necessary for PCET. An experimental design for a PCET study, in which an electron donor and acceptor are separated by a hydrogen-bonded interface, is shown in Figure 8. Since carboxylic acids have the ability to form cyclic dimers in low dielectric constant solvents, they were used as the hydrogen-bonded interface in the experiment.[167] The two

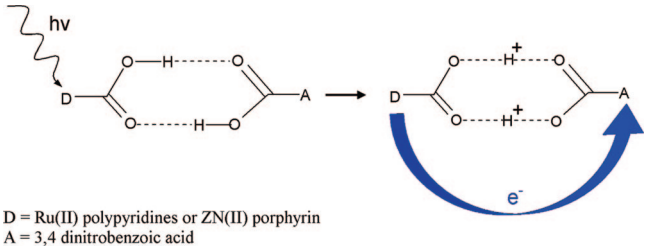

Figure 8. Donor (D) and acceptor (A) compounds for the PCET experiment. The photoinduced electron transfer from D to A induces symmetric double proton transfer between D and A. The symmetric hydrogen-bonded interface produces minor charge rearrangement due to double proton exchange.[167]

carboxylic acids were, respectively, substituted by an electron donor (ruthenium(II) polypyridines or zinc(II) porphyrin) and an organic electron acceptor such as 3,4-dinitrobenzoic acid.[167] In this study, the donor was photoexcited to initiate the PCET reaction. The pronounced kinetic isotope effect (KIE) of $k_H/k_D = 1.7$ and 1.6 for the charge separation and recombination rates provided the evidence of PCET reaction in the hydrogen-bonded network.

3.1. PCET Studies by Quantum Chemical Methods: Model Systems

3.1.1. Phenoxyl Radical−Phenol and Benzyl Radical−Toluene Complexes

Quantum chemical methods such as HF, DFT, and complete active space self-consistent field (CASSCF) have been used to study the PCET reactions.[65,168,169] These methods can provide good estimates of relevant kinetic and thermodynamic properties in PCET reactions. As a proton and electron transfer from a donor to an acceptor site in a system, the charge, spin, and MOs localized on the donor and acceptor sites change simultaneously. Thus, the calculation of the charge, spin, and plots of MOs along a reaction coordinate (transferring hydrogen or a proton) provides useful insight in understanding the PCET process. Mayer et al.[169] used B3LYP density functional and 6-31G* and 6-311G(2d,2p) basis sets to study PCET and HAT in (i) phenoxyl radical−phenol and (ii) benzyl radical−toluene. On the basis of the analysis of the singly occupied molecular orbital (SOMO) at a TS, the authors[169] identified the phenoxyl radical−phenol reaction as PCET and the benzyl radical−toluene reaction as HAT. For the phenoxyl radical−phenol system, the SOMO is localized on the 2p orbitals on donor and acceptor oxygen atoms that are perpendicular to the axis joining the two oxygen atoms (see Figure 9a) while the proton transfers along the hydrogen bond involving σ-MO. Since the electron and proton transfer through two different types of orbitals, the reaction was identified as PCET. In the benzyl radical−toluene system, the SOMO is localized along the direction joining the donor and acceptor (C···H···C) axes, and this was characterized as an HAT reaction (see Figure 9b). Using the state-averaged CASSCF(3,6) calculation, Hammes-Schiffer[168] also studied the phenoxyl radical−phenol and benzyl radical−toluene systems and supported the conclusions of Mayer et al.[169] Thus, on the basis of an examination of the plot of the SOMO, two types of reactions, PCET and HAT, were identified.

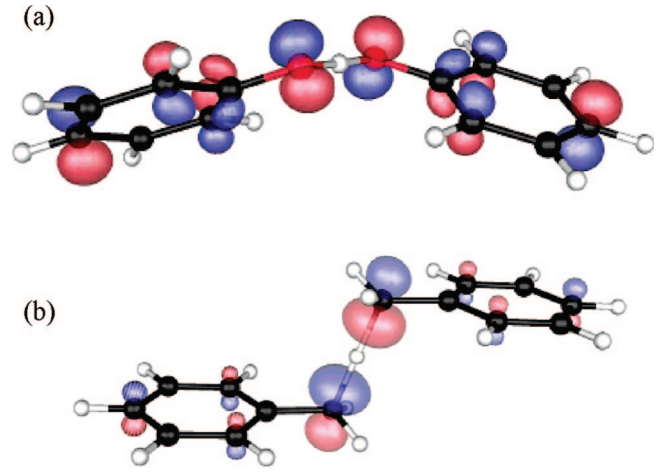

Figure 9. SOMO plot of (a) phenoxyl radical−phenol and (b) benzyl radical−toluene at the transition state structure. Reactions a and b are identified as PCET and HAT, respectively. Reprinted from ref 169. Copyright 2002 American Chemical Society.

3.1.2. Thymine−Acrylamide Radical Anion Complex

Acrylamide has a structure which is well suited to form hydrogen bonds with thymine in DNA. Studies on γ-irradiated acrylamide−DNA complexes at 77 K showed acrylamide is a poor electron scavenger; however, on thermal annealing to 130 K, electron transfer from DNA to acrylamide takes place with the apparent simultaneous formation of a neutral radical [$CH_3-CH^{(\bullet)}-CONH_2$) by proton transfer from the hydrogen-bonded thymine. The reaction clearly shows the involvement of PCET, as shown in Figure 10. The reaction of the radical anion of the thymine−acrylamide complex was theoretically studied by Sevilla and co-workers[170] using the B3LYP/6-31+G* density functional method. The optimized structures of the thymine−acrylamide radical anion complex and unpaired spin density distributions before and after proton transfer from thymine to acrylamide are shown in Figure 10. Before proton transfer, the spin density is localized on both thymine and acrylamide (Figure 10A). After proton transfer, the unpaired spin density is totally localized on acrylamide, which shows the involvement of PCET as suggested by the ESR experiment.[170]

In a subsequent work, the radical anions of thymine−acrylamide and DNA−acrylamide complexes were studied by Hammes-Schiffer and co-workers[171] using the CASSCF method using a frequency-resolved cavity model for the solvent based on the multistate continuum theory. The study showed that, for the solvated thymine−acrylamide radical anion complex, the electron transfer process dominates while, for the solvated DNA−acrylamide complex, PCET is involved. This difference was attributed to a decrease in the solvent accessibilities in the DNA, which changes the relative free energies of electron transfer and PCET product states.

4. PCET in One-Electron-Oxidized DNA Bases and Base Pairs

4.1. Guanine

The reversible deprotonation of one-electron-oxidized guanine ($G^{\bullet+}$) is a process of critical importance to the mediation of hole transfer within DNA. Experiments employing pulse radiolysis and 193 nm laser photolysis showed that one-electron-oxidized deoxyguanosine ($dG^{\bullet+}$) has a pK_a of 3.9 and deprotonates from its N_1H site (see Figure 11) in

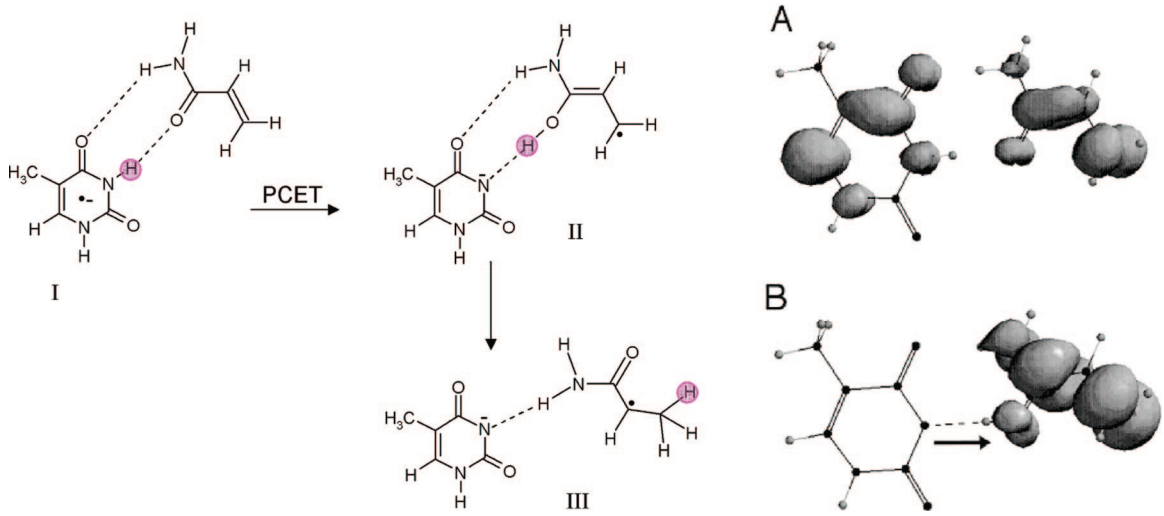

Figure 10. Optimized structures of thymine−acrylamide radical anion complexes, before and after proton transfer, and their spin density distributions. (A) DFT spatial spin distribution for species **I** (before proton transfer). Note that the spin is shared over both the thymine and acrylamide structures at an isodensity of 0.002 e Å^{-3}. (B) DFT spatial spin distribution for species **II** (after PCET) at an isodensity of 0.002 e Å^{-3}. The pink circle highlights the transferring proton. Reprinted from ref 170. Copyright 2001 American Chemical Society.

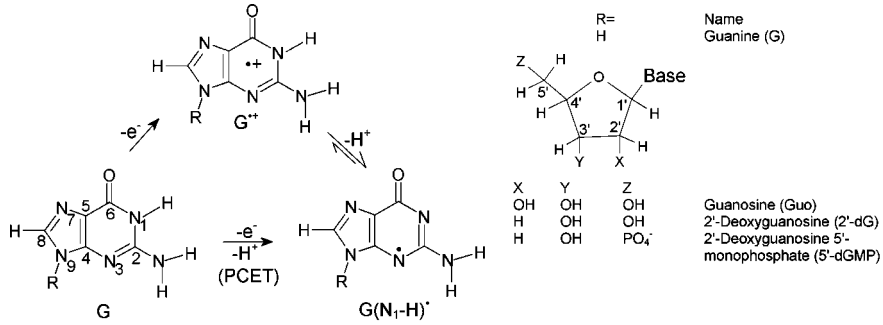

Figure 11. ET−PT (stepwise) and PCET reaction pathways for the oxidation of guanine.

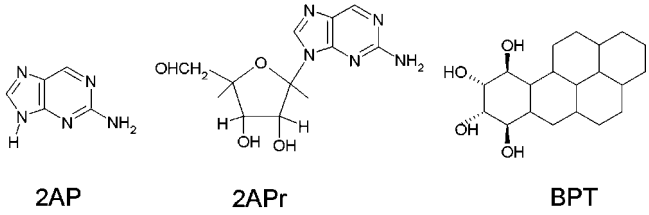

Figure 12. Structures of 2AP, 2APr, and BPT.[174,179]

an aqueous environment.[40,172,173] In aqueous solutions of DNA, production of guanine radical ($G(N_1H)^\bullet$) from guanine is possible through either a stepwise (ET−PT) or a concerted PCET reaction pathway as shown in Figure 11. In the PCET pathway, the reaction proceeds directly to the formation of a thermodynamically stable product ($G(N_1H)^\bullet$). The kinetic solvent isotope effects on the electron transfer kinetics associated with the oxidation of guanine in 5′-dGMP, DNA, and oligonucleotides by 2-aminopurine (2AP), 2-aminopurine ribose (2APr), and aromatic pyrenyl radical cations ($BPT^{\bullet+}$) (structures shown in Figure 12), employing laser flash photolysis transient absorption spectroscopy, have been studied by Shafirovich and co-workers.[52,174−179]

Photoexcitation of 2AP or 2APr in aqueous buffer solution (pH 7.0) with 308 nm XeCl excimer laser pulses results in the two-photon ionization of 2AP or 2APr:[52,174]

$$2AP \xrightarrow[\text{ionization}]{\text{308 nm laser pulse}} 2AP^{\bullet+} + e_h^- \qquad (4)$$

The radical cation ($2AP^{\bullet+}$ or $2APr^{\bullet+}$) rapidly deprotonates in the aqueous solution to give $2AP(-H)^\bullet$ or $2APr(-H^\bullet)$ neutral radicals:

$$2AP^{\bullet+} \xrightarrow{-H^+} 2AP(-H)^\bullet \qquad (5)$$

The reaction of these neutral radicals ($2AP(-H)^\bullet$ or $2APr(-H^\bullet)$) with 5′-dGMP results in the formation of 5′-$dGMP(-H)^\bullet$ neutral radical:

$$2AP(-H)^\bullet + 5'\text{-dGMP} \rightleftharpoons 2AP + 5'\text{-dGMP}(-H)^\bullet \qquad (6)$$

A pronounced kinetic isotope effect was observed on the kinetics of the oxidation of 5′-dGMP by $2AP(-H)^\bullet$ (or $2APr(-H^\bullet)$) in the H_2O and D_2O solutions from transient absorption measurements. The value of $k(H_2O)/k(D_2O)$ in the range 1.5−2.0 is evidence that the involvement of PCET through electron transfer from 5′-dGMP to $2AP(-H)^\bullet$ (or $2APr(-H^\bullet)$) radicals is coupled to the proton transfer from 5′-dGMP.[52,74] The oxidation of 5′-dGMP by $BPT^{\bullet+}$ was also carried out in a fashion similar to that above, and in this case too the PCET mechanism was proposed from the KIE value of ∼1.5.[175]

Subsequently, the electron transfer reactions between the guanine−guanine (GG) doublet (donor) and 2AP radical (acceptor) separated by intervening thymine or adenine bases in oligonucleotides and in DNA were studied using two-

Oligonucleotides[177]	dsDNA[176]
5'-2APTTTTTTTTTTTTTT-3'	5'-2APTTGGTTTTTTTTT-3'
5'-2APGGTTTTTTTTTTT-3'	5'-2APTTTGGTTTTTTTTT-3'
5'-2APTGGTTTTTTTTTT-3'	5'-2APAAAAAAGGAAAAAA-3'
5'-2APTTGGTTTTTTTT-3'	
5'-2APTTTGGTTTTTT-3'	
5'-2APTTTTGGTTTT-3'	
5'-2APAAAAGGAAAAAAAA-3'	

Figure 13. Design of 2AP-modified oligonucleotides and DNA duplexes used in refs 176 and 177.

Scheme 1. Oxidation of Guanine by 2AP(−H)• Subsequently Proceeds through Protonation and Deprotonation from Solvent and Results in G(−H)• Formation through PCET

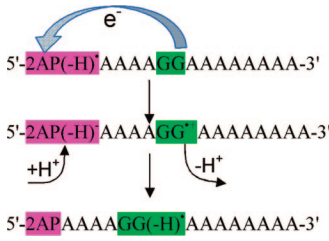

photon laser excitation.[176,177] The sequences used in the study are shown in Figure 13. The photoexcitation of 2AP-modified oligonucleotides (single- and double-stranded; see Figure 13) with 308 nm laser pulses results in the site-selective two-photon photoionization of the 2AP residue, which subsequently deprotonates to give 2AP(−H)• radical; see eqs 4 and 5. The oxidation of guanine by 2AP radicals was monitored by the evolution of the transient absorption spectra of 2AP radicals and guanine radicals. The oxidation of guanines by 2AP(−H)• and the formation of guanine radical (G(−H)•) occur within 0.1−500 μs and were proposed to proceed through a PCET mechanism as shown in Scheme 1.

The KIEs associated with the oxidation of guanine by 2AP in DNA duplexes were measured in H_2O and D_2O, respectively. The rate constant of the formation of G(−H)• in H_2O was found to be larger than that in D_2O, and the measured $k(H_2O)/k(D_2O)$ lies in the range 1.3−1.7. From KIE values, the reaction was proposed to involve PCET. However, Huynh and Meyer[54] in their review suggested that a simple PCET is not a feasible pathway in this reaction because the electron transfers a long distance (>10 Å) in DNA and could not couple with the proton of the guanine because of its short-range nature. They[54] suggested that this reaction may occur by a one-electron and two-proton ($1e^-/2H^+$) MSEPT pathway. In this pathway, the long-range electron transfer from guanine to 2AP(−H)• is coupled by two spatially separated protons, which occurs from the aqueous solvent; see Scheme 1. We note that in duplex DNA the initial deprotonation of $G^{\bullet+}$ is to cytosine, not the aqueous solution, and this adds additional complexity to the process.

Thorp and co-workers[53,180,181] used stopped-flow spectrophotometry and electrochemical methods to study the kinetics of the oxidation of guanine in 5′-dGMP, herring testes DNA (double-stranded), 2′-deoxyguanosine 5′-triphosphate, and the oligonucleotides d[5′-GCA GTA GCA TGT GAC GAG TCG] hybridized to its Watson−Crick complement and complexed with $Ru(bpy)_3^{3+}$ (bpy = 2,2′-bipyridine) in phosphate buffer at pH 7. The oxidation reaction of guanine by $Ru(bpy)_3^{3+}$, which leads to G(−H)• formation, is given as follows:

$$Ru(bpy)_3^{3+} + G \rightleftharpoons Ru(bpy)_3^{2+} + G^{\bullet+} \quad (7)$$

$$G^{\bullet+} \rightleftharpoons G(-H)^{\bullet} + H^+ \quad (8)$$

If eq 7 is rate limiting, the slope of the Marcus plot RT ln k_{ET} vs $E_{1/2}$(III/II (redox potential)) should be 0.5, but if eq 8 is rate limiting, the corresponding slope should be 1.0.[181] In their study, RT ln k_{ET} vs $E_{1/2}$ for reaction of guanine with different metal complexes $X(bpy)_3^{3+/2+}$ (X = Fe, Ru, and OS)[53,180] was plotted, a slope of 0.8 ± 0.2 was obtained, and PCET was invoked involving reactions 7 and 8. The rate of reaction of guanine oxidation was also measured in H_2O and D_2O, and KIE values of 2.1 and 1.4 were observed for DNA and mononucleotides, respectively. The study was extended to 7-deaza analogues of guanine and adenine in mononucleotide triphosphate forms, and a slope of the plot RT ln k_{ET} vs $E_{1/2}$ corresponding to 1.1 in each case was obtained. The KIEs with different metal complexes ranged from 2.2 to 10, respectively. Thus, the slope of >0.5 clearly indicates the involvement of a PCET mechanism in each of these systems. In this reaction, solvent acts as a proton acceptor, and thus, the reaction is likely an MSEPT.

The deprotonation preferred site of the guanine radical cation in aqueous solution is also considered in a few studies.[40,172,182−184] Pulse radiolysis experiments suggest the N_1H site for deprotonation in 2′-deoxyguanosine radical cation (2′-$dG^{\bullet+}$), while in 1-methylguanosine radical cation deprotonation must occur from the NH_2 group.[172,173,182] In aqueous solution, 2′-$dG^{\bullet+}$ and 1-methylguanosine radical cation have pK_a values of 3.9 and 4.7.[172] The pK_a of 1-methylguanosine radical cation is higher than that of 2′-$dG^{\bullet+}$ by 0.8 pH unit. Thus, while both the sites of $G^{\bullet+}$ are in competition for deprotonation in aqueous solution, the N_1H site is likely favored over N_2H. Recently, one-electron-oxidized 2′-dG by γ-irradiation at 77 K, ESR measurements, and theoretical calculations confirmed that the N_1H site is the preferred site for deprotonation of 2′-$dG^{\bullet+}$ in aqueous solution.[184]

4.1.1. Photooxidation of Guanine by Metal−Ligand Charge Transfer Complexes

$[Ru(TAP)_2(dppz)]^{2+}$ (TAP = 1,4,5,8-tetraazaphenanthrene, dppz = dipyrido[3,2-*a*:2′,3′-*c*]phenazine), shown in Figure 14, is a DNA intercalator and in its excited state becomes a highly oxidizing agent.[185,186] It not only oxidizes guanine in guanosine 5′-monophosphate (5′-GMP), but also guanine-containing polynucleotides $[poly(dG\text{-}dC)]_2$. Excitation of $[Ru(TAP)_2(dppz)]^{2+}$ is of the $\pi\pi^*$ type and results in a singlet excited state. Within picoseconds intersystem (singlet-to-triplet) crossing (ISC) takes place in aqueous solution at pH 7, as observed from UV/vis absorption data.[186] This triplet excited state arises due to metal−ligand (Ru−TAP) charge

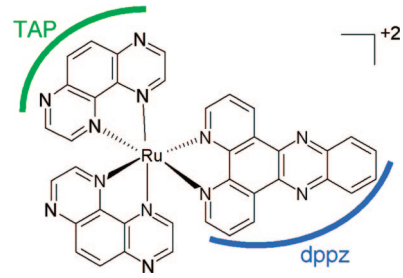

Figure 14. Structure of $[Ru(TAP)_2(dppz)]^{2+}$.[186]

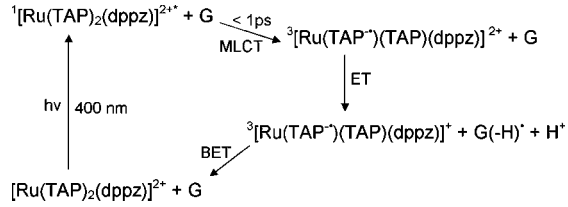

Figure 15. Formation of the MLCT excited state of $[Ru(TAP)_2(dppz)]^{2+}$ and ET from G to form G(−H)$^\bullet$ via PCET. See refs 185 and 186.

transfer (MLCT) and has a lifetime of several nanoseconds in aqueous solution. The oxidation of guanine by $[Ru(TAP)_2(dppz)]^{2+}$ in an excited triplet state is shown in Figure 15.

The reaction was carried out in both H_2O and D_2O, giving KIE values of 1.3 and 1.6 for forward and back electron transfer (BET), shown in Figure 15, and it was proposed that oxidation of guanine in the excited state is due to PCET or MSEPT. In the case of the G-C base pair, a proton transfers from G to C, while in 5′-GMP proton transfer is to the solvent. In this study, it was also proposed that a proton from G$^{\bullet+}$ may also transfer to the reduced parent complex $[Ru(TAP^{\bullet-})(TAP)(dppz)]^+ + G(-H)^\bullet + H^+ \rightarrow [Ru(TAP^\bullet(H))(TAP)(dppz)]^{2+} + G(-H)^\bullet$.

4.1.2. PCET in the Guanine−Cytosine (G-C) Base Pair

One-electron oxidation of the G-C base pair results in a transfer of a proton from N_1 of G to N_3 of cytosine as shown in Figure 16. In this context, proton transfer reactions in one-electron-oxidized double-stranded DNA oligonucleotides containing G, GG, and GGG sequences have been investigated using nanosecond pulse radiolysis experiments.[187,188] One-electron oxidation of guanine in double-stranded DNA was produced by $SO_4^{\bullet-}$.[172,187,188] It is also noted that the spectra of dG$^{\bullet+}$ and N_1-deprotonated dG(−H)$^\bullet$ are quite similar and absorb around 380 and 480 nm.[172,173,185,187,188] A weaker absorbance at ca. 625 nm was characterized as due to deprotonation of G$^{\bullet+}$ to G(−H)$^\bullet$.[187,188] Recent work in our laboratory suggests the absorption at 625 nm is likely from G(−H)$^\bullet$ with the proton loss to solvent from N_2. This we discuss further below. The kinetics of one-electron oxidation of guanine by $SO_4^{\bullet-}$ in deoxyguanosine (dG) and different DNA sequences was measured in H_2O and D_2O, respectively. The change in the absorbance at 625 nm after pulse radiolysis in H_2O and D_2O of dG and double-stranded oligonucleotide (5′-AAAAAGGGAAAAA-3′) is shown in Figure 17, and the corresponding KIE values of 1.7 and 3.5 were measured.

Double-stranded oligodeoxynucleotides containing 5-bromocytosine ($pK_a = 2.8$) and 5-methylcytosine ($pK_a = 4.7$) substitutions in the sequences were also investigated as they change the pK_a of cytosine ($pK_a = 4.3$) and were found to

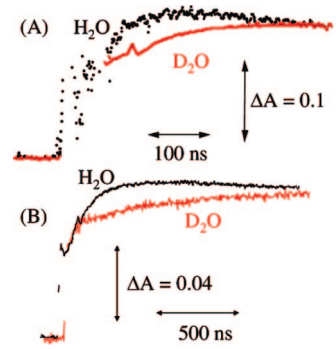

Figure 17. Absorbance changes at 625 nm after pulse radiolysis of dG (5.6 mM) (A) and double-stranded DNA (5′-AAAAAGG-GAAAAA-3′) (2.1 mM) (B) in the presence of ammonium persulfate (20 mM), NaCl (0.1 M), and *tert*-butyl alcohol (0.1 M) in 20 mM sodium phosphate in H_2O at pH 7 (black) or in D_2O at pD 7 (red). Reprinted from ref 188. Copyright 2008 American Chemical Society.

affect the rates of production of G(−H)$^\bullet$ as expected, with 5-bromocytosine having the lowest rate at 1.2×10^6 s^{-1}, cytosine having a rate of 8.7×10^6 s^{-1}, and 5-methylcytosine having the highest rate at 2.0×10^7 s^{-1}. However, all dsDNA oligomers with and without substitutions were found to have large KIEs for G(−H)$^\bullet$ formation of 3−3.5, whereas for the deoxynucleoside, dG, only 1.7 was found.[188] These large KIEs in oligonucleotides provide strong evidence that the deprotonation reaction of G$^{\bullet+}$ is a PCET. Further, in this study, the proton transfer from G$^{\bullet+}$ to C is strongly supported by the results found for substituted cytosines in dsDNA. A further step involving transfer to the solvent is also proposed, suggesting MSEPT.[188]

The protonation state and hole localization in one-electron-oxidized double-stranded DNA sequences were investigated very recently using ESR. The site of hole localization was determined by use of oligomers with deuterium substitution at the C_8 position of guanine (8-deuterioguanine (G^d)) at selected sites in the DNA sequences.[119] The work demonstrated that ESR spectra of one-electron-oxidized 8-deuterio-2′-deoxyguanosine (2′-dG$^{d\bullet+}$) and its deprotonated species (2′-dG(−H)$^{d\bullet}$) recorded at 77 K are distinguishable from each other; see Figure 18. The ESR spectra of 2′-dG$^{d\bullet+}$ and 2′-dG(−H)$^{d\bullet}$ were used as benchmark spectra for ESR analysis of one-electron-oxidized deuterated double-stranded DNA oligomers to characterize the protonation state of one-electron-oxidized guanine in the DNA oligomers. The ESR measurements for one-electron-oxidized double-stranded d[G^{d}CG^{d}CG^{d}CG^{d}C]$_2$ showed that one-electron-oxidized guanine exists as a neutral radical G(N_1H)$^\bullet$ in DNA; see Figure 18. Thus, at low temperatures only G(N_1H)$^\bullet$ is observed; however, this study pointed out that while proton transfer from guanine to cytosine in DNA is thermodynamically favored at ambient temperatures, owing to the small free

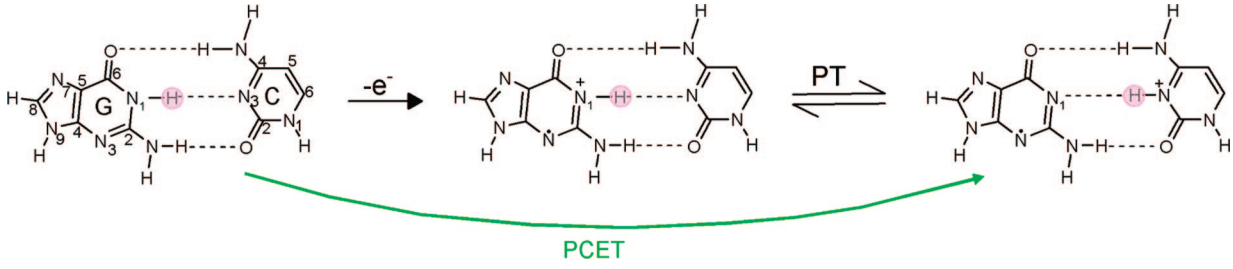

Figure 16. Scheme showing prototropic equilibria of proton transfer in the one-electron-oxidized G-C base pair. One-electron oxidation of the G-C base pair and proton transfer from G to C can occur from stepwise or concerted PCET within the DNA duplex.

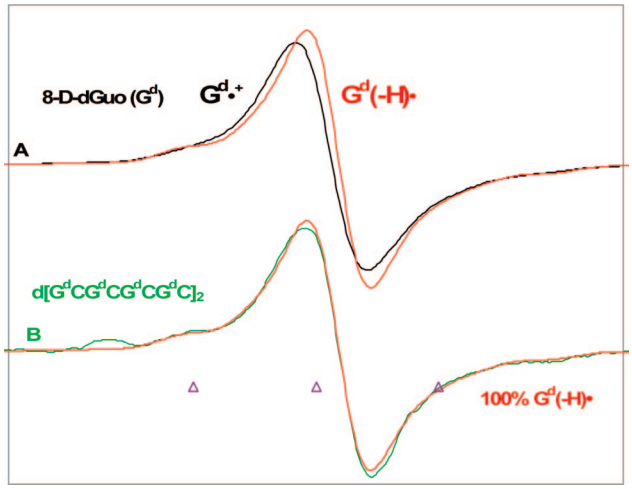

Figure 18. ESR spectra of (A) $G^{d\bullet+}$ (black) and $G^{d}(-H)^{\bullet}$ (red) obtained from glassy (7.5 M LiCl in D_2O) samples of G^d [G^d = 8-D-dGuo, 96% D] (3 mg/mL). (B) Spectrum of the one-electron-oxidized dsDNA oligomer $d[G^dCG^dCG^dCG^dC]_2$ (2 mg/mL) with $G^{d}(-H)^{\bullet}$ from (A) in red superimposed. The match of green and red spectra in (B) clearly shows that one-electron-oxidized guanine in the dsDNA oligomer exists as $G^{d}(-H)^{\bullet}$. One-electron oxidation of the monomer and the DNA oligomers was carried out via thermal annealing at 155 K. All spectra were recorded at 77 K. Adapted from ref 119. Copyright 2009 American Chemical Society.

energy difference, an equilibrium between the two forms (see Figure 16) is expected as predicted earlier by Steenken.[40]

Another interesting feature of this work is that by investigating dsDNA oligomers with G^d substitutions at specific sites the site of hole localization could be ascertained. For example, the oligomer $TG^dGGCCCA$ showed that most of the localization of the hole was at the $C_{5'}$ end of the GGG stack as had been predicted in earlier studies which relied on product analysis as well as by theoretical calculations. Although some hole localization at other sites (15−20%) was found, this was attributed to the small thermodynamic differences in energy between the various sites which only slightly favor the $C_{5'}$ site. No evidence for charge delocalization was found.

A number of other studies involving DNA systems are of note. Hole transfer rates in double-stranded DNA were also measured in H_2O and D_2O.[189] A decrease in charge transfer rate by a factor of 3 in D_2O was observed, which clearly shows the slower deuteron shift from $G^{\bullet+}$ to C compared to the corresponding proton shift. This KIE effect supports the coupling of hole transfer with intrastrand proton transfer in the DNA duplex.[189] Small KIEs of 1.2 and 1.3 for the double-stranded DNA sequence for hole transfer between naphthalimide (NI) and phenothiazine (PTZ) in its excited state were observed by Majima and co-workers.[190,191] Oxidation of guanine in DNA by $Ru(phen)_2(bpy)_3^{3+}$ using the flash-quench technique has been studied, and neutral guanine radical ($G(-H)^{\bullet}$) was detected by transient absorption spectroscopy and electron paramagnetic resonance (EPR).[147,192,193] Oxidation of guanine in the DNA duplex by $SeO_3^{\bullet-}$ and $SO_4^{\bullet-}$ ions generated by pulse radiolysis and the rapid formation of cytosine radical has been observed by transient absorption spectroscopy.[194] Using the first-principles quantum-mechanical and molecular-mechanics (QMMM) approach, molecular dynamics simulation on a fully hydrated 38-base-pair B-DNA d(5′-ACGCACGTCGCATAATATTACGTGGGTAT-TATATTAGC-3′) in the radical cation state showed that

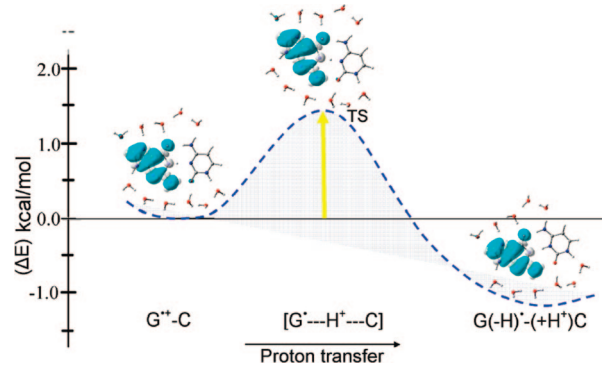

Figure 19. B3LYP/6-31+G**-calculated potential energy surface (PES) of PT in $G^{\bullet+}$-C in the presence of 11 waters with ZPE correction. Energy is given in kilocalories per mole. Spin density distributions during proton transfer are also shown. Reprinted from ref 200. Copyright 2009 American Chemical Society.

double proton transfer from guanine to cytosine can be coupled with the charge transfer.[195]

4.1.3. Thermodynamic Stability of $G^{\bullet+}$-C and $G(N_1H)^{\bullet}$-(+H^+)C

A number of theoretical investigations of the proton transfer reaction in a one-electron-oxidized guanine−cytosine base pair have been attempted.[195−199] In these computational studies, the transition state for the proton transfer from $G^{\bullet+}$ to C in the $G^{\bullet+}$-C base pair and the relative stabilities of $G^{\bullet+}$-C (reactant) and $G(N_1H)^{\bullet}$-(+H^+)C (product) (see Figure 16) were calculated in the gas phase, and the reaction was found to be endergonic by a few kilocalories per mole, which disfavors the proton transfer from $G^{\bullet+}$ to C in disagreement with experiment. In a more recent study,[200] the proton transfer reaction in $G^{\bullet+}$-C was modeled in the presence of 11 water molecules surrounding the G-C base pair (see Figure 19), and the reaction was found to be exothermic by 1.2 kcal/mol after zero-point energy (ZPE) correction. The calculated ZPE-corrected free energy (ΔG) of −0.65 kcal/mol at 298 K is in excellent agreement with experimental estimation of $\Delta G = -0.55$ kcal/mol, on the basis of the aqueous-phase pK_a values of $G^{\bullet+}$ and the C base.[42,199] The calculated spin densities are localized on the guanine moiety in agreement with experiment; see Figure 19. The greater thermodynamic stability of $G(N_1H)^{\bullet}$-(+H^+)C over $G^{\bullet+}$-C adds support to the involvement of PCET in any hole transfer by hopping within DNA.

4.1.4. PCET in the Excited State of the G-C Base Pair

A PCET excited-state deactivation mechanism for a G-C base pair within double-stranded DNA has been proposed from experiment and theory.[201−207] Sobolewski and Domcke[201,202] proposed a coupled electron proton transfer mechanism for the G-C base pair which is illustrated in Figure 20. In the ground state of the G-C base pair, the HOMO is localized on guanine while the LUMO is localized on cytosine. Photoexcitation of the G-C base pair initiates an electron transfer from the HOMO to the LUMO, which corresponds to a charge transfer (CT) excited state, designated as $^1\pi\pi^*$(CT) (blue curve); see Figure 20. In this charge transfer excited state, the N_1H proton of G transfers spontaneously to C without a barrier and crosses to the ground-state curve (pink color). Thus, the populated excited state returns to the ground state, and the normal G-C structure

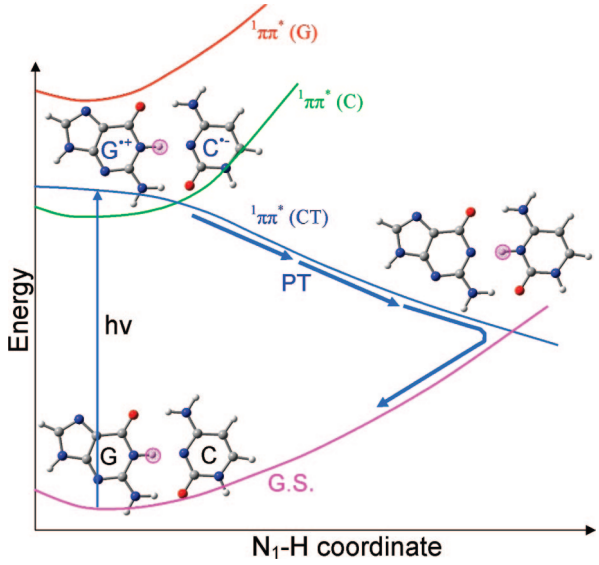

Figure 20. Sketch of the ultrafast excited-state deactivation pathway of the G-C base pair through the proton-coupled electron transfer mechanism.[201,202]

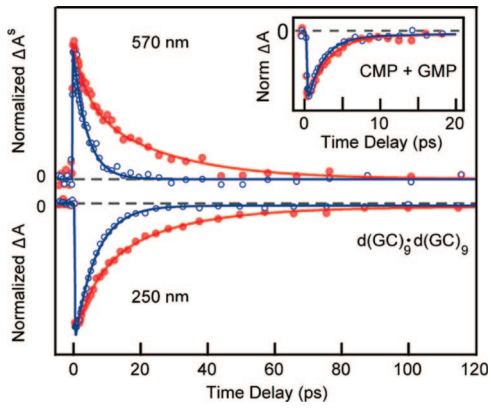

Figure 21. Normalized transient absorption signals showing (top) excited-state absorption and (bottom) ground-state bleach recovery of d(GC)$_9$·d(GC)$_9$ in H_2O (blue) and D_2O (red). The inset shows the 250 nm transient for an equimolar mixture of the monomers CMP and GMP in H_2O (blue) and D_2O (red). Reprinted from ref 207. Copyright 2009 American Chemical Society.

is restored. This PCET mechanism is supported by molecular dynamics simulations and experiment.[203−207]

Very recently, Kohler and co-workers[207] investigated the deuterium isotope effect on the excited-state dynamics of G-C-containing DNA duplexes using transient absorption spectroscopy. This study demonstrated a pronounced isotope effect on the excited-state lifetimes in an alternating G-C oligonucleotide. For a d(GC)$_9$·d(GC)$_9$ oligonucleotide, the transient absorption signals were recorded at 266 nm with probe wavelengths of 250 and 270 nm in H_2O and D_2O. The results evidence a faster ground-state recovery for d(GC)$_9$·d(GC)$_9$ in H_2O than in D_2O; see Figure 21. However, for 5′-GMP and 5′-CMP the KIE is very modest; see the inset of Figure 21. In this study the authors also come to the conclusion that the formation of exciplex states with significant CT character enables intrabase pair proton transfer in DNA which decays with a PCET mechanism as described in Figure 20.

4.1.5. Repair of Guanyl Radical (G(N$_1$H)$^•$) through PCET

A series of studies have employed γ-irradiated aqueous solutions of plasmid DNA samples in the presence of thiocyanate to generate guanyl radicals (G(N$_1$H)$^•$). The sites of guanine radical formation are detected after formation of the products 8-oxo-G and fapyG (2,6-diamino-4-hydroxy-5-formamidopyrimidine). *Escherichia coli* base excision repair endonucleases are used to convert these stable end products to single- and double-strand breaks in the plasmids which are readily detected and distinguished using gel electrophoresis.[208−210] In these works,[208−210] it has been shown that the strand breaks can be strongly attenuated if micromolar concentrations of substituted phenols, indoles, or anilines are present. These phenols are able to reduce the guanyl radical, which subsequently accepts a proton from phenol. On the basis of the energetics involved for stepwise ET and PT pathways and the concerted PCET pathway (see Figure 6 in section 3), it was concluded that the repair of guanyl radical occurs by PCET as shown in the following equation:

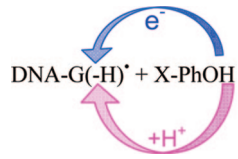

(9)

The repair mechanism of deprotonated DNA bases (B$^{•+}$ → B(−H)$^•$ + H$^+$; B = A, T, G, and C) by thiols was investigated by theoretical calculations.[211] The results showed that the repair of A(−H)$^•$ and C(−H)$^•$ should be favored via PCET at any pH while, for G(−H)$^•$ and T(−H)$^•$, a PCET process is preferred at acidic to neutral pH values. In the pH range of 9−11, the ET pathway would dominate. The repair of G(N$_1$H)$^•$ and its anion (G(N$_1$H)$^-$) by amino acids (cysteine and tyrosine) was also proposed to involve hydrogen atom transfer and PCET.[212]

4.2. Cytosine and Thymine

Deprotonation reactions of one-electron-oxidized cytosine (C$^{•+}$) and thymine (T$^{•+}$) (shown in Figure 22) have been studied in a number of papers.[213−217] The radical cation of 5-methylcytosine produced in aqueous glasses by UV photolysis at 77 K was found to deprotonate from the methyl group upon warming at 190 K, as evidenced from ESR measurements.[213,214] Similarly, the oxidation of thymine at 77 K by photoionization and ESR spectra showed the formation of similar deprotonated species, UCH$_2^•$ (methyl-deprotonated thymine cation radical).[215] In another study,[216] photoexcitation of anthraquinone-2,6-disulfonic acid (2,6-AQDS) with cytosine by a 308 nm XeCl excimer laser oxidizes cytosine by electron transfer from cytosine to 2,6-AQDS in the triplet state via interstate (singlet-to-triplet) crossing. The oxidized cytosine deprotonates from its N$_1$ site.[216] If cytosine is replaced by 1-methylcytosine, deprotonation occurs from the NH$_2$ group of the cytosine. The radicals were directly detected by time-resolved Fourier-transform EPR in H_2O and D_2O at 10 °C on the nanosecond time scale,[216] while the formation of the radical cation was not detected. The reaction mechanism along with the structure of 2,6-AQDS is shown in Scheme 2.

Very recently, one-electron oxidation in the single crystals of cytosine monohydrate doped with a very small amount

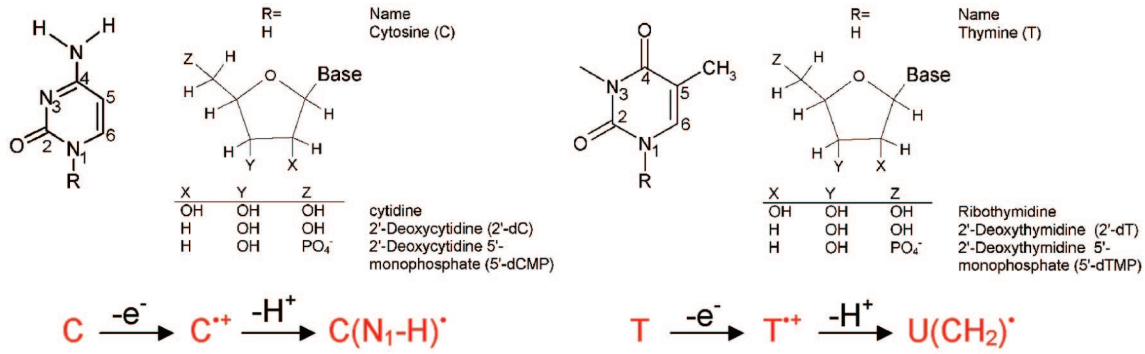

Figure 22. Typical deprotonation reactions of one-electron-oxidized cytosine and thymine.

Scheme 2. One-Electron Oxidation of Cytosine via PCET[a]

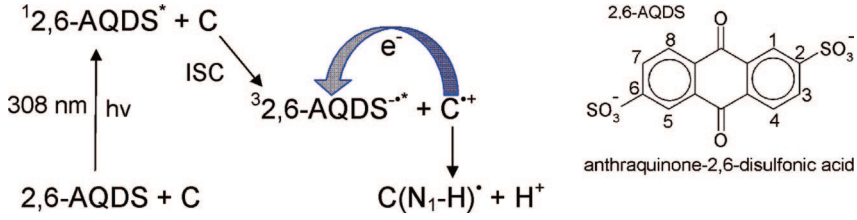

[a] See ref 216.

of 2-thiocytosine was carried out by X-irradiation.[217] The radicals formed between 10 and 150 K after oxidation in normal and partially deuterated samples were investigated by EPR spectroscopy. A huge KIE ($>10^2-10^3$) at 100 K indicates that radical formation occurs via a proton-coupled electron/hole transfer (PCET/PCHT) mechanism. The hydrogen bonds between cytosines in the crystals provide a ready minimum energy path for proton transfer. In the X-irradiated doped crystals both anion and cation radicals of cytosine are initially formed. The one-electron-oxidized cytosine ($C^{\bullet+}$) subsequently transfers a hole to 2-thiocytosine because of its lower ionization potential compared to that of cytosine.[217] Thus, 2-thiocytosine acts as a hole acceptor at 10 K in these crystals. Finally, one-electron-oxidized 2-thiocytosine deprotonates to a hydrogen-bonded cytosine. Theoretical calculations show that only when hole transfer is combined with a proton transfer (PT1) does the reaction become exothermic. The schematic diagram for the PCHT reaction is shown in Scheme 3. The hole/electron recombination reaction activated at 60 K also was suggested to involve PCET.

Scheme 3. Formation of the Thiocytosine Deprotonated Cation by PCHT[a]

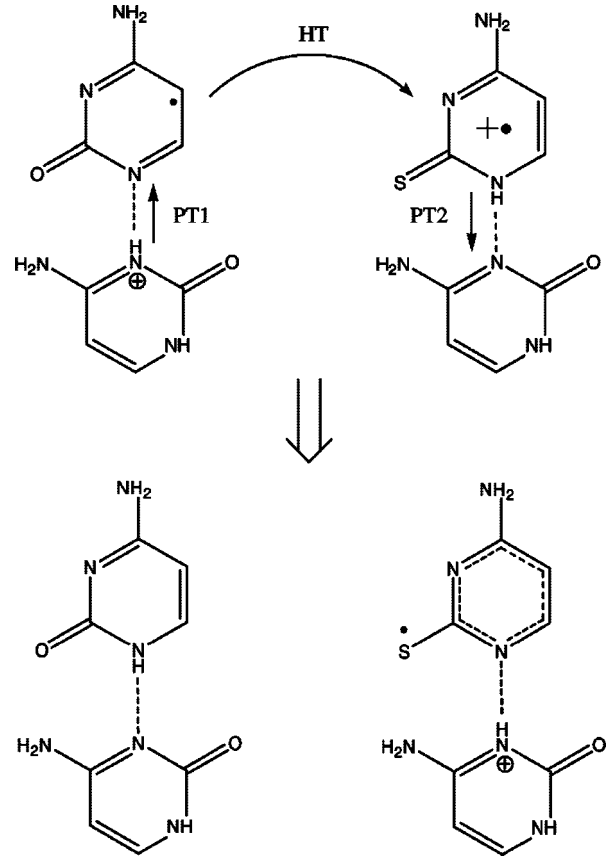

[a] Reprinted from ref 217. Copyright 2008 American Chemical Society.

4.3. Adenine

The absorption spectrum of one-electron oxidation of adenine in 2′-deoxyadenosine (dA) by $SO_4^{\bullet-}$ in aqueous solution was studied by Steenken.[40] The resulting absorption spectrum of $dA^{\bullet+}$, measured between pH 0 and pH 6, showed the existence of $dA(-H)^{\bullet}$ produced by deprotonation at the NH_2 group of the adenine cation radical;[40] see Figure 23. From the absorption spectrum, it was concluded that the pK_a of $dA^{\bullet+}$ in aqueous solution is <1. The $dA(-H)^{\bullet}$ formation from $dA^{\bullet+}$ was also supported by ESR and electron nuclear double resonance (ENDOR) studies of X-irradiated dAdo crystals at 10 K,[218] pulse radiolysis experiments in aqueous solution,[219] and ESR studies of γ-irradiated dA.[220] While $dA^{\bullet+}$ is experimentally found to produce the neutral radical ($dA(-H)^{\bullet}$) in an aqueous environment, the oxidation of adenine stacks in DNA oligomers was observed to be metastable to deprotonation.[220] This observation was reported in a recent ESR study of one-electron oxidation by $Cl_2^{\bullet-}$ of adenine in dA and in stacked DNA oligomers $(dA)_6$ as a function of pH.[220] The stability of one-electron-oxidized

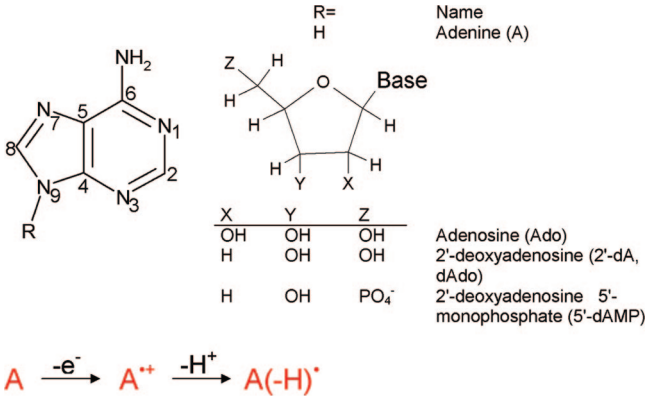

Figure 23. Deprotonation of one-electron-oxidized adenine.

adenine stacks in DNA was attributed to a charge delocalization mechanism which inhibits the deprotonation of $A^{\bullet+}$ and may facilitate the observed long-range charge transfer process through A stacks in DNA. These experiments strongly suggest that deprotonation would strongly attenuate large-range hole transfer and greatly slow PCET.

4.3.1. Adenine-Thymine (A−T) Base Pair

Steenken[40] considered the proton transfer on one-electron oxidation of an A-T base pair from the NH_2 group of adenine to the O_4 atom on thymine (see Figure 24) and suggested from experimental data that such a transfer should be unfavorable. A theoretical treatment of this proton transfer reaction for the ground state of the hydrogen-bonded A-T base pair radical cation has been reported for the gas phase.[198] From the calculation of the relative stabilities of $A^{\bullet+}$-T (reactant) and $A(-H)^{\bullet}$-(H^+)T (product), the reaction was found to be endothermic by 1.2 kcal/mol,[198] which disfavors the proton transfer as predicted earlier by Steenken.[40] The inclusion of aqueous media would be helpful in future efforts. The excited states of the A-T base pair using the CC2 (simplified singles and doubles coupled cluster) method were treated recently.[221] The calculated excited-state PES for proton transfer from adenine to thymine in the $^1\pi\pi^*$(CT) (charge transfer excited state) showed that the deactivation process of the excited A-T base pair is driven by the PCET mechanism[221] as shown in section 4.1.4 for the G-C base pair.

4.4. Sugar Radical Formation through PCET

In addition to DNA base radicals, sugar radicals are also formed due to ionization and γ-irradiation of DNA,[35−39] which ESR experiments suggest account for about 7−15% of trapped radicals at low temperatures.[39b] These sugar radicals are known to produce unaltered base release and associated single-strand breaks in DNA. The formation of sugar radicals through the abstraction of a hydrogen atom from the sugar ring by $OH^{\bullet}$ and the direct oxidation of the sugar−phosphate backbone followed by deprotonation is well documented in the literature.[35,37] The direct formation of a sugar radical by photoexcitation of radical cations of guanine

Scheme 4. Formation of the Neutral Sugar Radical ($C_{5'}^{\bullet}$) through a Proton-Coupled Electron Transfer Mechanism in 2′-Deoxyguanosine Radical Cation ($dG^{\bullet+}$)[a]

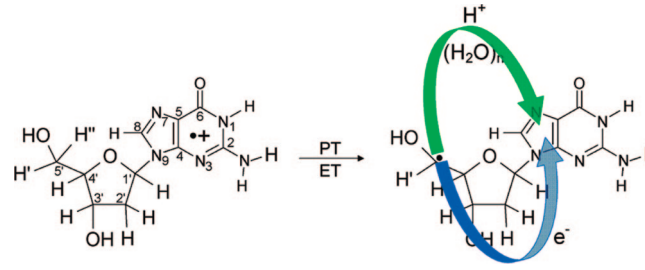

[a] The proton transfers from $C_{5'}$ to N_7 of guanine through water molecules and results in electron transfer from $C_{5'}$ to guanine, yielding the product $dG(^{\bullet}C_{5'},N_7H^+) + 7H_2O$. Reprinted from ref 228. Copyright 2009 American Chemical Society.

$(G^{\bullet+})$ and adenine $(A^{\bullet+})$ in model systems of deoxyribonucleotides, ribonucleotides, and DNA and RNA oligomers has been proposed recently in a number of studies.[36,39,222−226] The underlying mechanism of sugar radical formation proposed in these studies[36,39,222−226] is that photoexcitation induces hole transfer from the one-electron-oxidized DNA base to the sugar ring, which is followed by rapid deprotonation $(-H^+)$ at specific carbon sites on the sugar ring, which prevents the back transfer of the hole to the base.[37,38,227] The hole transfer from the base to sugar is, of course, accompanied by an electron transfer from the sugar to the one-electron-oxidized base. Thus, the overall sugar radical formation process is clearly a PCHT (or PCET) as depicted in Scheme 4.[228]

The involvement of PCET/PCHT in the sugar radical formation from $dG^{\bullet+}$ in the presence of seven water molecules was explored using the density functional theory.[228] In these calculations, the PES for the $C_{5'}$ radical formation was calculated by stretching the $C_{5'}$−H bond in $dG^{\bullet+}$ in the presence of water molecules employing the B3LYP/6-31G* level of theory. At each step of $C_{5'}$−H bond elongation (proton transfer) on the PES, the spin densities were also calculated to observe the electron transfer process; see Figure 25. The study clearly demonstrates that only a slight increase in the $C_{5'}$−H bond length of 0.13 Å is sufficient to reach the transition state and completely transfer the spin initially localized on the guanine base in $dG^{\bullet+}$ (step 1 in Figure 25) to the $C_{5'}$ site on the deoxyribose (sugar) group (step 2 in Figure 25). Beyond the TS the proton ultimately transfers to N_7 of guanine (step 6 in Figure 25) through the intervening water molecules without any significant barrier. The proton transferred $(dG(^{\bullet}C_{5'},N_7H^+) + 7H_2O)$ (product, step 6) is found to be ca. 13 kcal/mol more stable than the reactant $dG^{\bullet+} + 7H_2O$ (reactant, step 1). Very small deuterium isotope effects of 1.5 ± 0.3 and 1.3 ± 0.3 were observed for the formation of $C_{5'}^{\bullet}$ and $C_{3'}^{\bullet}$, respectively, from 2′-deoxyguanosine radical cation at 143 K,[223] which according to Hammond's postulate[229] shows that the geometries of the TS and reactant are likely to be close to each other. The theoretical calculations strongly support this

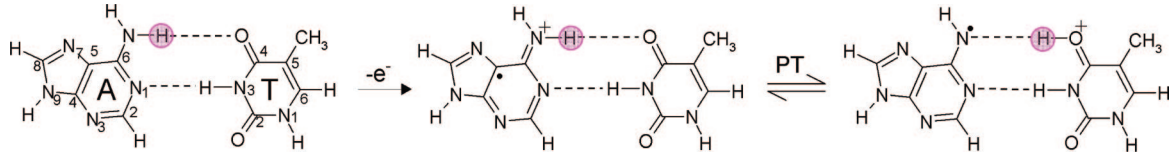

Figure 24. Scheme showing prototropic equilibria of proton transfer in the one-electron-oxidized A-T base pair.

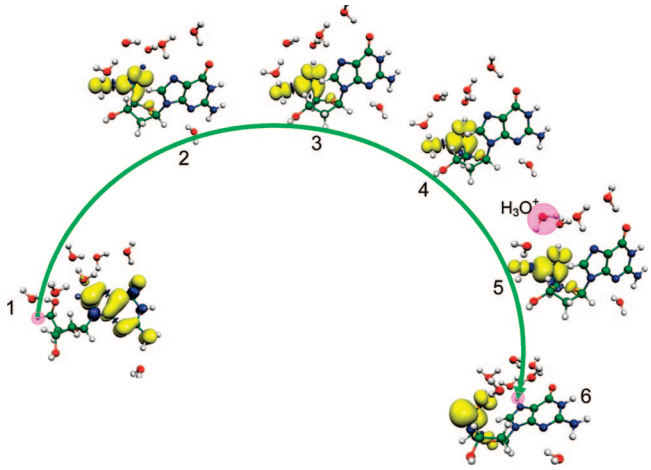

Figure 25. BHandHLYP/6-31G*//B3LYP/6-31G*-calculated spin density distribution during proton transfer from $C_{5'}$ on the deoxyribose group to the N_7 site on guanine in $dG^{\bullet+} + 7H_2O$ (step 1). The stretching of the $C_{5'}$−H bond from its equilibrium bond length (1.099 Å) to 1.23 Å (TS) (steps 1 and 2) results in the complete transfer of the hole from guanine to the $C_{5'}$ site, which is equivalent to electron transfer from the $C_{5'}$ site to guanine. The pink circle highlights the transferring proton when not obscured by the spin distribution. Reprinted from ref 228. Copyright 2009 American Chemical Society.

conclusion. Clearly, the direct formation of sugar radicals from $G^{\bullet+}$ necessitates the involvement of PCET.

5. PCET in One-Electron-Reduced DNA Bases and Base Pairs

The electron attachment process involves one-electron reduction of a molecule (M) and leads to molecular radical anion formation ($M^{\bullet-}$). The energetic stability of $M^{\bullet-}$ is given by the electron affinity (EA) of the molecule. Electron transmission spectroscopy (ETS)[230] and anion photoelectron spectroscopy[231] experiments showed that the vertical and adiabatic EAs of conventional DNA bases (A, T, G, and C) in the gas phase are negative (<0) or near zero. In competition with valence anion formation in the gas phase, bases such as T and U with significant dipole moments can bind the free electron near the molecular framework with a weak interaction typically less than 0.1 eV. Such species are called dipole-bound anions and are not considered relevant to DNA in condensed media. However, in an aqueous environment, the solvation energy increases the electron affinity of the bases by several electronvolts and stable valence radical anions are formed for all the DNA bases. These valence DNA base anion radicals are quite basic and usually react by protonation at heteroatom sites (N and O) (reversibly) as well as carbon sites (irreversibly) to form stable neutral radicals. These species are observed from ESR, pulse radiolysis, and photoelectron spectroscopy experiments. Below we give several examples of these studies.

5.1. Guanine

Single crystals of N_7-protonated guanine in guanine hydrochloride dehydrate X-irradiated at 20, 65, and 150 K were studied by ESR/ENDOR techniques.[232,233] The study showed one-electron reduction of the guanine−HCl results in a neutral species which undergoes protonation at O_6 to restore the one-electron-reduced guanine to its original charge state at 20 K. The species starts as a molecular cation (N_7-protonated guanine), and on one-electron reduction the neutral intermediate forms, which protonates at O_6, restoring the species to the initial charge state as a radical cation. The authors[232] found that this is a general mechanism for one-electron-reduced species which undergo protonation to restore the original charge state and one-electron-oxidized species which undergo deprotonation to the original charge state within the crystalline lattice.[233] This mechanism was initially proposed by Bernhard.[234] The crystalline Coulombic stabilization is likely a factor; however, in aqueous solutions the same processes take place because the electron adducts and one-electron-oxidized species become far more basic and acidic, respectively.

Wang and Sevilla[235] investigated various A, T, G, and C systems and observed irreversible protonations at carbon at every base under specific conditions. For example, they observed C_8-protonated guanine radical anion ($G(C_8H)^{\bullet}$) by ESR of γ-irradiated frozen aqueous solutions of dGMP·dCMP, polyG·polyC, and poly[dG]·poly[dC] samples. However, for DNA systems with A and T present no protonation of the guanine radical anion is found.

The reactions of hydrated electrons with guanosine (Guo), 2′-deoxyguanosine (2′-dG), and 1-methylguanosine were studied by pulse radiolysis in aqueous solution with optical and conductometric detection.[236] At pH 7, the reduction of dG was completed in <0.1 μs, and protonation initially occurred at N_7 of $dG^{\bullet-}$, which was observed by an increase in the absorption spectra at 300 nm. Tautomerization, from N_7 to C_8, resulting in the irreversibly protonated neutral radical of $dG^{\bullet-}$, was proposed to result as shown in the following equations:

$$dG \xrightarrow{+\,e_{aq}^-} dG^{\bullet-} \qquad (10)$$

$$dG^{\bullet-} + H_2O \longrightarrow dG(NH)^{\bullet} + OH^- \qquad (11)$$

$$dG(NH)^{\bullet} \xrightarrow{\text{tautomerization}} dG(C_8H)^{\bullet} + OH^-$$

$$dG(C_8H)^{\bullet} + H^+ \rightleftharpoons dG(C_8H)H^{\bullet+} \qquad (12)$$

The OH^- produced in eq 11 is neutralized by H^+ to form H_2O as confirmed from the conductance measurement with $k = 1.4 \times 10^{11}$ M^{-1} s^{-1}. At pH < 6, $dG(C_8H)^{\bullet}$ is further protonated to give the radical cation, eq 12. The rate of nitrogen protonation at 300 nm (eq 11) was also monitored in D_2O, and KIE = 8.0 was observed, which demonstrated the rate-determining step was reaction 11 for the proton transfer to C_8 of guanine.

The valence-bound radical anion of guanine was also studied by Bowen and his collaborators using photoelectron spectroscopy and theory.[237−239] Figure 26 shows the photoelectron spectrum of $G^{\bullet-}$ measured with 3.493 eV photons. The spectrum of $G^{\bullet-}$, shown in Figure 26, has two maxima, one ranging from 0.8 to 1.1 eV and the other steeply increasing from 2.4 to 3.2 eV. This broad-band nature of the spectra suggested the presence of several tautomers of $G^{\bullet-}$ that arise as a result of intramolecular proton transfer to carbon sites.[237] The presence of tautomers was supported by theoretical calculations at the B3LYP and CCSD(T) levels of theory.[237−239] This study provides good evidence for electron-induced internal proton transfer reactions. The

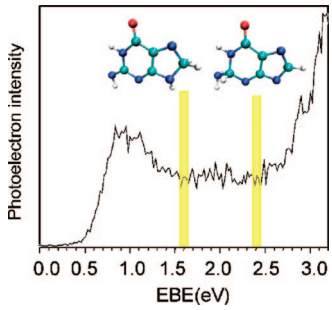

Figure 26. Photoelectron spectrum of $G^{\bullet-}$ measured with 3.493 eV photons. The electron-induced proton-transferred structures (tautomers of $G^{\bullet-}$) present at 1.6 and 2.4 eV are shown. At 1.6 eV, a proton transfers from the NH_2 group to C_8, and at 2.4 eV a proton transfers from N_9 to C_2 of guanine. For numbering, see Figure 11. Reprinted from ref 237. Copyright 2007 American Chemical Society.

calculated photoelectron energies at 1.6 and 2.4 eV are for the two tautomer structures of $G^{\bullet-}$ shown in Figure 26.

Very recently, one-electron reduction of 8-bromoisoguanosine and 8-bromoxanthosine anion were investigated in aqueous media using pulse radiolysis techniques and theory.[240] From theory and experiments, it was proposed that electron-induced protonation of 8-bromoisoguanosine and 8-bromoxanthosine (monoanion) occurs through ET−PT (stepwise) and concerted PCET mechanisms.

5.1.1. Proton Transfer in the One-Electron-Reduced G-C Base Pair

Intra base pair proton transfer, induced by electron attachment to G-C base pairs, has been observed by pulse radiolysis[241] in solution and photoelectron spectroscopy[242] gas-phase experiments. These experimental works were strongly supported by a number of theoretical[196,199,243−246] studies.

Tagawa and co-workers[241] measured the dynamics of one-electron-reduced single- and double-stranded oligonucleotides containing G and C sequences spectroscopically via nanosecond pulse radiolysis in aqueous solution. The addition of a hydrated electron (e_{aq}^-) to the oligonucleotide results in transfer to cytosine in a G-C base pair. The cytosine anion radical ($C^{\bullet-}$) rapidly protonates at N_3 by transfer from N_1 of the hydrogen-bonded guanine. The equilibrium constant for this reaction was estimated to be 3.16×10^3, suggesting a nearly complete proton transfer.

The gas-phase photoelectron spectrum of the radical anion of 9-methylguanine−1-methylcytosine ($MGMC^{\bullet-}$) was recorded using 3.94 eV photons by Bowen and co-workers;[242] see Figure 27. The photoelectron spectrum of $MGMC^{\bullet-}$ shows a broad peak in the energy range from ca. 1.4 to 2.5 eV having a maximum intensity near 2 eV; see Figure 27. The broad nature of the spectrum shows the presence of several tautomers of $MGMC^{\bullet-}$. From theory, the presence of two types of $MGMC^{\bullet-}$ were characterized: (i) normal $MGMC^{\bullet-}$ in the Watson−Crick conformation, shown on the left in Figure 27, and (ii) proton transferred from the N_1 atom of guanine to the N_3 atom of cytosine, shown on the right in Figure 27. This experiment establishes the involvement of electron-induced proton transfer events in the G-C base pair.

A number of detailed theoretical investigations have treated the proton transfer reaction in the one-electron-reduced G-C base pair.[196,199,243−246] In each of these studies, the PES for N_1H proton transfer from guanine to N_3 of cytosine was

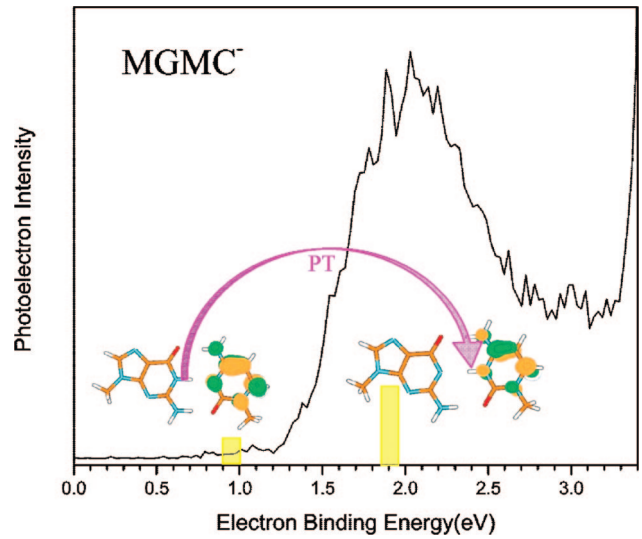

Figure 27. Photoelectron spectrum of the $MGMC^{\bullet-}$ recorded with 3.49 eV photons. The left structure is $MGMC^{\bullet-}$ in Watson−Crick conformation. The right structure is due to proton transfer from the N_1 site of guanine to the N_3 site of cytosine. Reprinted from ref 242. Copyright 2009 American Chemical Society.

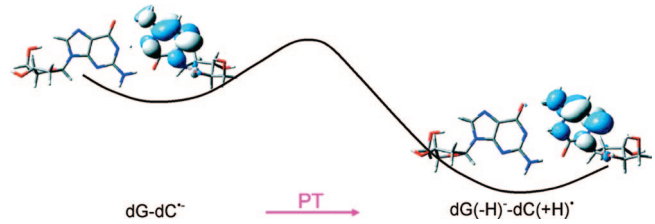

Figure 28. SOMOs for the nucleoside pair dG-$dC^{\bullet-}$ and proton-transferred $dG(-H)^-$-$dC(+H)^{\bullet}$. $dG(-H)^-$-$dC(+H)^{\bullet}$ is 2.3 kcal/mol more stable than dG−$dC^{\bullet-}$ calculated by the B3LYP/DZP++ method.[244] Reprinted with permission from ref 244. Copyright 2007 American Institute of Physics.

calculated and the proton transfer reaction was found to be exothermic by several kilocalories per mole. The PES for proton transfer along with the SOMO plots, calculated with the B3LYP/DZP++ method by Schaefer and co-workers,[244] is shown in Figure 28. Experiment and theory thus support the involvement of PCET in the one-electron-reduced G-C base pair.

5.2. Cytosine and Thymine

Neutral radicals of cytosine and thymine (shown in Figure 29) are formed on protonation of one-electron-reduced cytosine and thymine bases and their 2′-nucleosides and 2′-nucleotides. Each of these species has been detected by ESR[213−215,247−249] and pulse radiolysis[41,241,250,251] experiments. Pulse radiolysis[41,241] and conductance measurements[250] have shown that, in the pH range 6−13, one-electron reduction of cytosine results in the N_3-protonated cytosine radical ($C(N_3H)^{\bullet}$). The N_3-protonated species has a pK_a near 13, so it is not surprising that the formation of $C(N_3H)^{\bullet}$ from $C^{\bullet-}$ is rapid, ≤20 ns, as shown in Figure 29. EPR/ENDOR spectroscopy[248b] of X-irradiated cytosine monohydrate ($C \cdot H_2O$) single crystals at 10 K has also shown the presence of $C(N_3H)^{\bullet}$. In addition, the formation of the C_6-protonated species has been observed in ESR experiments, which likely stems from $C(N_3H)^{\bullet}$.[235]

$T(O_4H)^{\bullet}$ and $T(C_6H)^{\bullet}$ radicals have been detected by ESR[213−215,247,248a] and pulse radiolysis[41,241] experiments on

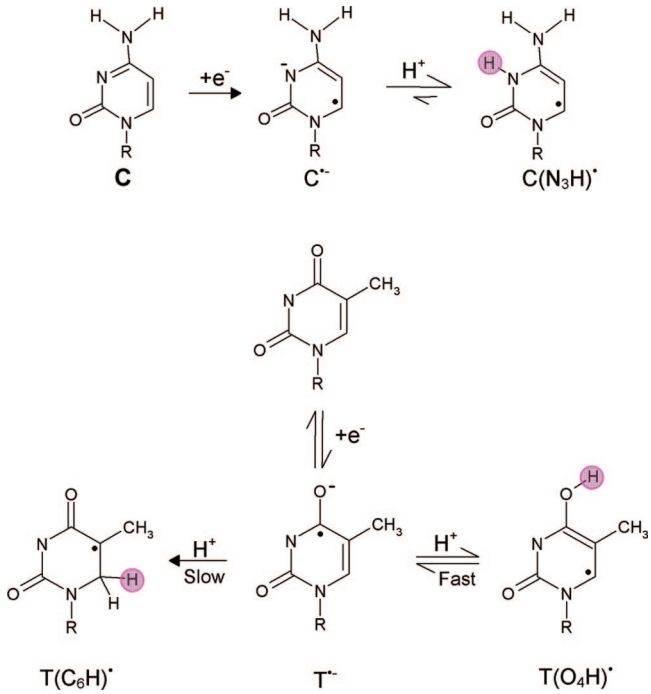

Figure 29. Neutral radical formation from one-electron-reduced cytosine and thymine bases (R = H, deoxyribose (phosphate)). The water acts as a proton (H^+) donor. The site of protonation is shown by a pink circle.

protonation of one-electron-reduced thymine, dT, and dTMP as shown in Figure 29. The protonation at O_4 is reversible,[41,241] whereas the protonation at C_6 is irreversible.[213−215,247,248a] The spectra recorded 1 μs after the pulse[241] showed the presence of $T(O_4H)^•$ and $T^{•-}$ at pH 3.5 and 10.5. The transiently formed $T^{•-}$ was directly protonated by the water, and at pH 7, the rate constant for the O_4 protonation was estimated to be 4.3×10^5 s^{-1}.[241] Proton transfer from water in the X-irradiated thymine monohydrated ($T•H_2O$) crystal was also proposed from EPR spectroscopy.[252] These early studies based on pulse radiolysis and ESR/EPR experiments also support that protonation of cytosine and thymine is induced by the attachment of an excess electron to the bases. Both cytosine and thymine anion radicals undergo irreversible protonation at carbon (shown for thymine only) as a slower step than the reversible protonation at the heteratom.[235]

5.2.1. PCET in the Excited State of Pyrene-Modified Pyrimidine Nucleosides

Steady-state fluorescence spectroscopy and femtosecond time-resolved transient absorption spectroscopy[253] have been used to investigate the DNA-mediated reductive electron transfer employing 5-(pyren-1-yl)-2′-deoxyuridine (PydU) and 5-(pyren-1-yl)-2′-deoxycytidine (PydC), structures shown in Figure 30, as model nucleosides for DNA.

The excitation of the pyrene moiety in PydU and PydC leads to electron transfer (charge transfer excited state) from the pyrene moiety to uracil and cytosine, yielding $Py^{•+}$, $U^{•-}$, and $C^{•-}$ formation.[253,254] The excitation was carried out in the presence of acetonitrile (MeCN) and in water at different pH values to investigate the protonation state of $dU^{•-}$ and $dC^{•-}$. The result showed that $dC^{•-}$ was protonated spontaneously, see Scheme 5, even in the basic aqueous solution within picoseconds as expected from its strongly basic pK_a of 13. The fast protonation of dC directly from the local excited (LE) state ($Py^*dC + H^+$) occurs through the PCET

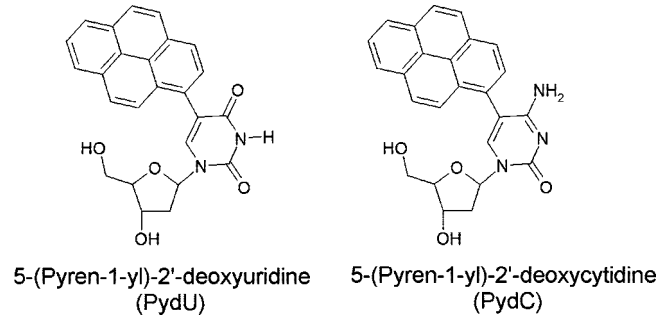

Figure 30. Structures of PydU and PydC.[253]

Scheme 5. PCET Process in the Excited State of PydC[a]

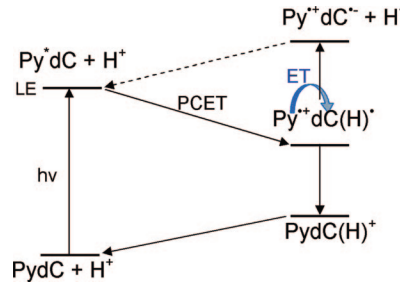

[a] Adapted from ref 253. Copyright 2004 Wiley-VCH.

process. However, the thermodynamically unstable CT excited state ($Py^{•+}dC^{•-} + H^+$) occurs at high pH by deprotonation of $Py^{•+}dC(H)^•$ and clearly lies higher in energy than the initial LE state.

The effect of the base sequence on excess ET in various polynucleotide duplexes and salmon sperm DNA was studied in frozen glassy aqueous solutions (7 M LiBr in D_2O) of the duplexes polydAdT•polydAdT and polydIdC•polydIdC (dI = inosine) randomly intercalated with mitoxantrone (MX) by Sevilla and co-workers.[122,255] In this study only a modest kinetic isotope effect was observed for DNA on the electron transfer rate, 0.83 ± 0.1 $Å^{-1}$ (H_2O) vs 0.92 ± 0.1 $Å^{-1}$ (D_2O). However, the rate of electron transfer in polydAdT•polydAdT, 0.7 $Å^{-1}$, was substantially faster than in polydIdC•polydIdC, 1.4 $Å^{-1}$. This was attributed to the fact that proton transfer readily occurs from I to C anion radical and greatly slows the electron transfer process; however, for the A-T polynucleotide, no such transfer process occurs and the electron transfer rate is unhindered. This result was supported by theoretical calculations that show the proton transfer in the I-C base pair anion radical from I to C is barrierless.[199]

Proton transfer reactions in radical anions of 1-methylcytosine and uracil in the gas phase and in solvation were also investigated by Harańczyk et al.[256−258] using theory. In these studies, the relative stabilities of various tautomers of 1-methylcytosine and uracil radical anions were investigated using DFT, MP2, and CCSD(T) methods. On the basis of stabilities, the most stable tautomer, formed by intramolecular proton transfer, was proposed to be present. For the radical anion of uracil complexed with alcohols, it was found that the excess electron attachment to the complex (uracil−alcohol) induces a barrier-free proton transfer from the OH group of the alcohol to the O_4 atom of uracil. This theoretical prediction was supported by the photoelectron spectra.

Scheme 6. Hydrated Electron (e_{aq}^-) Induced Protonation of the Adenine Base (A) in Adenosine at Nitrogen and Carbon Sites[260]

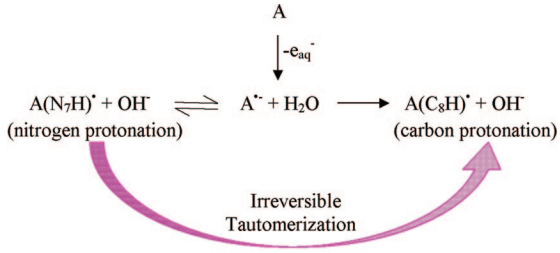

5.2.2. Protonation of One-Electron-Reduced Adenine and A-T Base Pair

Pulse radiolysis and optical dc conductivity measurements found that attachment of an excess hydrated electron (e_{aq}^-) to adenosine (Ado) and dAMP is followed by proton transfer to the adenine from water within 1 ns, as shown in Scheme 6.[259,260] At pH 7, the nitrogen-protonated dA(N$_7$H)$^\bullet$ is converted into carbon-protonated dA(C$_8$H)$^\bullet$ by an irreversible tautomerization with a rate constant of 2×10^6 M^{-1} s^{-1}.[260] This result shows that electron attachment to adenine is coupled with the intermolecular proton transfer from solvent, which could be described as PCET.

Recently, barrier-free proton transfer induced by an excess electron attachment to monomers of adenine, adenosine 5′-monophosphate, and 2′-deoxyadenosine 5′-monophosphate and adenine complexed with formic acid was investigated using photoelectron spectroscopy in the gas phase along with theory.[261−264] Further, the proton transfer from adenine to thymine in the one-electron-reduced A-T base pair was proposed from the photoelectron spectra and the theoretical calculation,[265] though the predicted base pair structure does not correspond to the canonical Watson−Crick base pair. This is not surprising considering these are gas-phase systems.

5.2.3. Electron-Induced DNA Strand Break Formation in Excited States

Recent advances in several laboratories have shown that the interaction of low-energy electrons (LEEs) with DNA is of significant biological importance. Since the discovery by Sanche and co-workers that LEEs < 4 eV (below the ionization threshold of DNA) can induce single- and double-strand breaks,[20,266,267] the problem of elucidating the mechanism of strand breaks in DNA has been extensively treated in theoretical investigations[268−273] and by experiment.[20−27,266,267] From experiments and theoretical calculations, two mechanisms were proposed. In the first, LEEs are initially captured by the base into their π^*-MOs to create a shape resonance (transient negative ion (TNI)) and the electron is transferred to the sugar phosphate region, leading to strand breaks. The second mechanism is direct attachment to the sugar phosphate backbone in higher energy empty (virtual) orbitals, leading to dissociative electron attachment (DEA) and associated strand breaks.

The ground-state theoretical calculations, considering 5′-thymidine monophosphate (5′-dTMPH) radical anion as a model of DNA, calculated the PES for the strand breaks ($C_{5'}-O_{5'}$ bond). These works report the barrier height for $C_{5'}-O_{5'}$ bond dissociation in the range 10−19 kcal/mol, showing a quite small rate ($10^{10}-10^{-4}$ s^{-1})[269] is expected for $C_{5'}-O_{5'}$ bond cleavage. Recently, the excited state of the

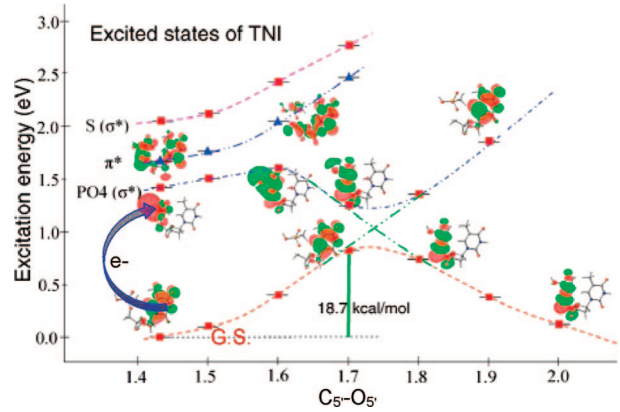

Figure 31. Lower curve: PES of the 5′-dTMPH TNI, calculated in the neutral optimized geometry of 5′-dTMPH with $C_{5'}-O_{5'}$ bond elongation. The SOMO is shown at selected points. Upper curves: calculated vertical excitation energies of the radical anion at each point along the PES. MOs involved in excitations are also shown. Energies and distances are given in electronvolts and angstroms, respectively. The lowest $\pi\pi^*$ state (triangles) and lowest $\pi\sigma^*$ states (square) are shown. Reprinted from ref 272. Copyright 2008 American Chemical Society.

TNI of 5′-dTMPH was calculated using the BHandHLYP/6-31G* method,[272] and the excited-state potential energy surfaces for $C_{5'}-O_{5'}$ bond dissociation were calculated as shown in Figure 31. In the calculation, the negative charge of the phosphate group of 5′-dTMPH was neutralized by protonating one of the oxygens of the phosphate group. From Figure 31, it is evident that, at an excitation energy of 1.4 eV, the electron transfers from thymine to the PO_4 region and this transition is $\pi\sigma^*$ in nature as suggested by the first mechanism proposed above. This transition is dissociative in nature and is predicted to lead to facile formation of strand breaks by cleavage of the $C_{5'}-O_{5'}$ bond; see Figure 31.

A more complex mechanism involving an excess electron attachment to the base followed by a proton attachment to the base and the subsequent attachment of another electron, inducing strand breaks and base release, is also proposed by both Dąbkowska et al.[231,274] and Gu et al.[231,275] using MPW1K/6-31+G** and B3LYP/DZP++ levels of theory. 3′-dCMP and 5′-dCMP were considered as models for the calculations.

6. Overview and Conclusion

The exposure of high-energy radiation to DNA initially forms ion radicals within DNA that quickly undergo proton transfer reactions. The resultant species undergo transfer within DNA by either (i) proton-coupled hole or (ii) proton-coupled electron transfer. These species transfer to sites where products are subsequently formed. The initial proton transfers occur because formation of holes or addition of an electron to the nucleobase strongly affects the pK_a values of the nucleobases, changing them by orders of magnitude. Oxidized DNA bases become substantially more acidic, while reduced DNA bases become more basic often by more than 5 pK_a units.[40] This acquired acid/base character of DNA bases gives rise to protonation/deprotonation reactions. Radiation-induced proton transfer often provides the energetic driving force for electron or hole transfer within DNA and between hydrogen-bonded base pairs in DNA. Remarkably, as described in this review, the reactions observed in aqueous solutions, crystalline solids, and the gas phase are often quite similar owing to the large driving forces involved after ion

radical formation. After the PCET process is complete the new stabilized species is clearly resistant to subsequent transfer unless the proton transfer process is reversible or a subsequent more exergonic reaction takes place. For example, within DNA, proton transfer processes may hinder both hole and electron transfer. For the hole which localizes predominantly on guanine in the GC radical cation base pair an equilibrium between $G^{\bullet+}$-C and $G(N_1H)^{\bullet}$-$C(+H^+)$ is established with a slight favoring of the proton-transferred species ($G(N_1H)^{\bullet}$-$C(+H^+)$) as the free energy difference between the two forms is small. At room temperature, an equilibrium between nearly equal amounts of $G^{\bullet+}$-C and $G(N_1H)^{\bullet}$-$C(+H^+)$ is established, which allows the hole to transfer. Excess electrons in DNA localize at both T and C, but proton transfer only occurs in the $G\text{-}C^{-\bullet}$ base pair and strongly favors the proton transfer state, $G(N_1H)^{-}$-$CH^{\bullet}$. This results in a redistribution of the initial distribution of the excess electron from both T and C to predominantly on C. This should create a strong base sequence dependence on electron transfer, favoring A-T sequences, and limits rapid transfer rates in G-C sequences to those processes and distances which can take place before proton transfer. As described in this review, these and other proton-coupled electron transfer processes are common in DNA after radical ion formation.

Finally, we note that there is a growing awareness that excited states combined with ion radicals are potent initiators of chemical events which include PCET. Excited states themselves create driving forces for hole and electron transfer which when combined with existing holes and excess electrons potentiate rapid reactive events such as hole transfer from the DNA base guanine to the sugar phosphate backbone discussed earlier. For the excess electron pathway, excited states are significant as well. For example, low-energy electron interactions with DNA can create in effect an excited-state anion radical if the attachment is in an MO above the LUMO. Calculations described above show that excited ion radical species are especially prone to inducing rapid cleavage of the DNA backbone.

Clearly, PCET events initiated by radiation damage to DNA have provided and will continue to provide a fertile ground for research seeking to understand the initial complex processes which are critical to understanding the ultimate biological effects of radiation.

7. Abbreviations

2AP	2-aminopurine
2Apr	2-aminopurine ribose
2′-dG^d	8-deuterio-2′-deoxyguanosine
2,6-AQDS	anthraquinone-2,6-disulfonic acid
5′-dTMP	5′-thymidine monophosphate
A	adenine
A-T	adenine−thymine base pair
BET	back electron transfer
bpy	2,2′-bipyridine
C	cytosine
$C(N_3H)^{\bullet}$	N_3-protonated cytosine radical
CASSCF	complete active space self-consistent field
CT	charge transfer
DFT	density functional theory
dG	deoxyguanosine
$dG^{\bullet+}$	one-electron-oxidized 2′-deoxyguanosine or 2′-deoxyguanosine radical cation
dI	inosine
dppz	dipyrido[3,2-*a*:2′,3′-*c*]phenazine
EA	electron affinity
e_{aq}^-	hydrated electron
ENDOR	electron nuclear double resonance
EPR	electron paramagnetic resonance
ESR	electron spin resonance
ET	electron transfer
ETS	electron transmission spectroscopy
fapyG	2,6-diamino-4-hydroxy-5-formamidopyrimidine
G	guanine
$G^{\bullet+}$	guanine radical cation
G-C	guanine−cytosine base pair
$G^{\bullet+}$-C	one-electron-oxidized guanine−cytosine base pair
G^d	8-deuterioguanine
$G(N_1H)^{\bullet}$	guanyl radical
H^-	hydride
HAT	hydrogen atom transfer
HF	Hartree−Fock
HOMO	highest occupied molecular orbital
IP	ionization potential
KIE	kinetic isotope effect
LEE	low-energy electron
LUMO	lowest unoccupied molecular orbital
MGMC	9-methylguanine−1-methylcytosine
MLCT	metal−ligand charge transfer
MO	molecular orbital
MSEPT	multisite electron and proton transfer
MX	mitoxantrone
NI	naphthalimide
PCET	proton-coupled electron transfer
PCHT	proton-coupled hole transfer
PES	potential energy surface
ps	picosecond
PT	proton transfer
PTZ	phenothiazine
PydC	5-(pyren-1-yl)-2′-deoxycytidine
PydU	5-(pyren-1-yl)-2′-deoxyuridine
SOMO	singly occupied molecular orbital
T	thymine
TAP	1,4,5,8-tetraazaphenanthrene
$T(C_6H)^{\bullet}$	C_6-protonated thymine radical
$T(O_4H)^{\bullet}$	O_4-protonated thymine radical
TNI	transient negative ion
TS	transition state
$UCH_2^{\bullet}$	methyl-deprotonated thymine radical cation

8. Acknowledgments

This work was supported by NIH NCI Grant No. R01CA045424. We thank Dr. Amitava Adhikary for helpful discussions and suggestions.

9. References

(1) Russell, P. *iGenetics*; Benjamin Cummings: New York, 2001.
(2) Saenger, W. *Principles of Nucleic Acid Structure*; Springer-Verlag: New York, 1984.
(3) von Sonntag, C. *The Chemical Basis of Radiation Biology*; Taylor and Francis: London, New York, Philadelphia, 1987.
(4) Swiderek, P. *Angew. Chem., Int. Ed.* **2006**, *45*, 4056, and references therein.
(5) Turecek, F. *Adv. Quantum Chem.* **2007**, *52*, 89.
(6) Lukin, M.; de los Santos, C. *Chem. Rev.* **2006**, *106*, 607.
(7) Becker, D.; Sevilla, M. D. *Adv. Radiat. Biol.* **1993**, *17*, 121.
(8) Tomkinson, A. E.; Vijayakumar, S.; Pascal, J. M.; Ellenberger, T. *Chem. Rev.* **2006**, *106*, 687.
(9) Close, D. M. In *Radiation Induced Molecular Phenomena in Nucleic Acids*; Shukla, M. K., Leszczynski, J., Eds.; Challenges and Advances in Computational Chemistry and Physics, Vol. 5; Leszczynski, J., Ed.; Springer Science + Business Media B.V.: Dordrecht, The Netherlands, 2008; pp 493−529.
(10) Swarts, S. G.; Sevilla, M. D.; Becker, D.; Tokar, C. J.; Wheeler, K. T. *Radiat. Res.* **1992**, *129*, 333.
(11) Li, X.; Sevilla, M. D. *Adv. Quantum Chem.* **2007**, *52*, 59.

(12) Becker, D.; Adhikary, A.; Sevilla, M. D. In *Charge Migration in DNA*; Chakraborty, T., Ed.; Springer-Verlag: Berlin, Heidelberg, 2007; pp 139−175.
(13) Kumar, A.; Sevilla, M. D. In *Radiation Induced Molecular Phenomena in Nucleic Acids*; Shukla, M. K., Leszczynski, J., Eds.; Challenges and Advances in Computational Chemistry and Physics, Vol. 5; Leszczynski, J., Ed.; Springer Science + Business Media B.V.: Dordrecht, The Netherlands, 2008; pp 577−617.
(14) Kumar, A.; Sevilla, M. D. In *Radical and Radical Ion Reactivity in Nucleic Acid Chemistry*; Greenberg, M., Ed.; John Wiley & Sons, Inc.: New York, 2010; pp 1−40.
(15) Becker, D.; Sevilla, M. D. In *Electron Paramagnetic Resonance*; Gilbert, B. C., Davies, M. J., Murphy, D. M., Eds.; Royal Society of Chemistry Specialist Periodical Report, Vol. 21; Royal Society of Chemistry: London, 2008; p 33.
(16) Yokoya, A.; Shikazono, N.; Fujii, K.; Urushibara, A.; Akamatsu, K.; Watanabe, R. *Radiat. Phys. Chem.* **2008**, *77*, 1280.
(17) Sevilla, M. D.; Becker, D.; Yan, M.; Summerfield, S. R. *J. Phys. Chem.* **1991**, *95*, 3409.
(18) Faraggi, M.; Ferradini, C.; JayGerin, J. P. *New J. Chem.* **1995**, *19*, 1203.
(19) International Commission on Radiation Units and Measurements (ICRU). ICRU Report No. 31; ICRU: Washington, DC, 1979.
(20) Boudaïffa, B.; Cloutier, P.; Hunting, D.; Huels, M. A.; Sanche, L. *Science* **2000**, *287*, 1658.
(21) Sanche, L. *Chem. Phys. Lett.* **2009**, *474*, 1.
(22) Sanche, L. In *Radical and Radical Ion Reactivity in Nucleic Acid Chemistry*; Greenberg, M., Ed.; John Wiley & Sons, Inc.: New York, 2010; pp 239−293.
(23) Zheng, Y.; Cloutier, P.; Hunting, D. J.; Sanche, L.; Wagner, J. R. *J. Am. Chem. Soc.* **2005**, *127*, 16592.
(24) Ptasińska, S.; Sanche, L. *Phys. Chem. Chem. Phys.* **2007**, *9*, 1730.
(25) Sulzer, P.; Ptasińska, S.; Zappa, F.; Mielewska, B.; Milosavljevic, A. R.; Scheier, P.; Märk, T. D.; Bald, I.; Gohlke, S.; Huels, M. A.; Illenberger, E. *J. Chem. Phys.* **2006**, *125*, 044304.
(26) (a) Bald, I.; Dąbkowska, I.; Illenberger, E. *Angew. Chem., Int. Ed.* **2008**, *47*, 8518. (b) Baccarelli, I.; Gianturco, F. A.; Grandi, A.; Sanna, N.; Lucchese, R. R.; Bald, I.; Kopyra, J.; Illenberger, E. *J. Am. Chem. Soc.* **2007**, *129*, 6269.
(27) Bernhard, W. A. *J. Phys. Chem.* **1989**, *93*, 2187.
(28) Hush, N. S.; Cheung, A. S. *Chem. Phys. Lett.* **1975**, *34*, 11.
(29) Orlov, V. M.; Smirnov, A. N.; Varshavsky, Ya. M. *Tetrahedron Lett.* **1976**, *17*, 4315.
(30) Yang, X.; Wang, X.-B.; Vorpagel, E. R.; Wang, L.-S. *Proc. Natl. Acad. Sci. U.S.A.* **2004**, *101*, 17588.
(31) Steenken, S.; Jovanovic, S. V. *J. Am. Chem. Soc.* **1997**, *119*, 617.
(32) Burrows, C. J.; Muller, J. G. *Chem. Rev.* **1998**, *98*, 1109.
(33) (a) Cadet, J.; Douki, T.; Ravanat, J.-L. *Acc. Chem. Res.* **2008**, *41*, 1075. (b) Cadet, J.; Douki, T.; Gasparutto, D.; Ravanat, J.-L. *Mutat. Res.* **2003**, *531*, 5.
(34) Swarts, S. G.; Gilbert, D. C.; Sharma, K. K.; Razskazovskiy, Y.; Purkayastha, S.; Naumenko, K. A.; Bernhard, W. A. *Radiat. Res.* **2007**, *168*, 367.
(35) Pogozelski, W. K.; Tullius, T. D. *Chem. Rev* **1998**, *98*, 1089.
(36) (a) Becker, D.; Bryant-Friedrich, A.; Trzasko, C.; Sevilla, M. D. *Radiat. Res.* **2003**, *160*, 174. (b) Shukla, L. I.; Pazdro, R.; Huang, J.; DeVreugd, C.; Becker, D.; Sevilla, M. D. *Radiat. Res.* **2004**, *161*, 582. (c) Shukla, L. I.; Pazdro, R.; Becker, D.; Sevilla, M. D. *Radiat. Res.* **2005**, *163*, 591.
(37) Adhikary, A.; Kumar, A.; Sevilla, M. D. *Radiat. Res.* **2006**, *165*, 479.
(38) Bernhard, W. A. In *Radical and Radical Ion Reactivity in Nucleic Acid Chemistry*; Greenberg, M., Ed.; John Wiley & Sons, Inc.: New York, 2010; pp 41−68.
(39) (a) Sharma, K. K.; Purkayastha, S.; Bernhard, W. A. *Radiat. Res.* **2007**, *167*, 501. (b) Purkayastha, S.; Milligan, J. R.; Bernhard, W. A. *Radiat. Res.* **2006**, *166*, 1.
(40) Steenken, S. *Chem. Rev.* **1989**, *89*, 503.
(41) Steenken, S.; Telo, J. P.; Novais, H. M.; Candeias, L. P. *J. Am. Chem. Soc.* **1992**, *114*, 4701.
(42) Steenken, S. *Biol. Chem.* **1997**, *378*, 1293.
(43) Tommos, C.; Tang, X.-S.; Warncke, K.; Hoganson, C. W.; Styring, S.; McCracken, J.; Diner, B. A.; Babcock, G. T. *J. Am. Chem. Soc.* **1995**, *117*, 10325.
(44) Okamura, M. Y.; Feher, G. *Annu. Rev. Biochem.* **1992**, *61*, 861.
(45) Hoganson, C. W.; Babcock, G. T. *Science* **1997**, *277*, 1953.
(46) Diner, B. A.; Babcock, G. T. In *Advances in Photosynthesis: The Light Reactions*; Ort, D. R., Yocum, C. F., Eds.; Kluwer Academic Publishers: Dordrecht, The Netherlands, 1996; Vol. 4, p 213.
(47) Blomberg, M. R. A.; Siegbahn, P. E. M.; Styring, S.; Babcock, G. T.; Akermark, B.; Korall, P. *J. Am. Chem. Soc.* **1997**, *119*, 8285.
(48) Hoganson, C. W.; Lydakis-Simantiris, N.; Tang, X.-S.; Tommos, C.; Warncke, K.; Babcock, G. T.; Diner, B. A.; McCracken, J.; Styring, S. *Photosynth. Res.* **1995**, *47*, 177.
(49) Babcock, G. T.; Wikstrom, M. *Nature* **1992**, *356*, 301.
(50) Malmstrom, B. G. *Acc. Chem. Res.* **1993**, *26*, 332.
(51) Siegbahn, P. E. M.; Eriksson, L.; Himo, F.; Pavlov, M. *J. Phys. Chem. B* **1998**, *102*, 10622.
(52) Shafirovich, V.; Geacintov, N. E. *Top. Curr. Chem.* **2004**, *237*, 129.
(53) Thorp, H. H. *Top. Curr. Chem.* **2004**, *237*, 159.
(54) Huynh, M. H. V.; Meyer, T. J. *Chem. Rev.* **2007**, *107*, 5004.
(55) Meyer, T. J.; Huynh, M. H. V.; Thorp, H. H. *Angew. Chem., Int. Ed.* **2007**, *46*, 5284.
(56) Thorp, H. H. *Chem. Abstr. Inorg. Chem.* **1991**, *3*, 171.
(57) Lui, W.; Thorp, H. H. *Excited-State Proton Transfer Reactions of Multiply-Bonded Ligands*; Advances in Transition Metal Coordination Chemistry, Vol. 1; JAI Press: Greenwich, CT, 1996; p 187.
(58) Roth, J. P.; Yoder, J. C.; Won, T.-J.; Mayer, J. M. *Science* **2001**, *294*, 2524.
(59) Mayer, J. M.; Rhile, I. J. *Biochim. Biophys. Acta−Bioenerg.* **2004**, *1655*, 51.
(60) Tommos, C.; Babcock, G. T. *Acc. Chem. Res.* **1998**, *31*, 18.
(61) Stubbe, J.; Nocera, D. G.; Yee, C. S.; Chang, M. C. Y. *Chem. Rev.* **2003**, *103*, 2167.
(62) Boussicault, F.; Robert, M. *Chem. Rev.* **2008**, *108*, 2622.
(63) Costentin, C. *Chem. Rev.* **2008**, *108*, 2145.
(64) Cukier, R. I.; Nocera, D. G. *Annu. Rev. Phys. Chem.* **1998**, *49*, 337.
(65) Hammes-Schiffer, S.; Iordanova, N. *Biochim. Biophys. Acta* **2004**, *1655*, 29.
(66) Hammes-Schiffer, S. *ChemPhysChem* **2002**, *3*, 33.
(67) Hammes-Schiffer, S. *Acc. Chem. Res.* **2009**, *42*, 1881.
(68) Hammes-Schiffer, S. *Acc. Chem. Res.* **2001**, *34*, 273.
(69) Hammes-Schiffer, S. *Acc. Chem. Res.* **2006**, *39*, 93.
(70) Hammes-Schiffer, S. Proton-coupled electron transfer. In *Electron Transfer in Chemistry. Vol. I. Principles, Theories, Methods and Techniques*; Balzani, V., Ed.; Wiley-VCH: Weinheim, Germany, 2001; p 189.
(71) Chang, C. J.; Chang, M. C. Y.; Damrauer, N. H.; Nocera, D. G. *Biochim. Biophys. Acta−Bioenerg.* **2004**, *1655*, 13.
(72) Himo, F.; Siegbahn, P. E. M. *Chem. Rev.* **2003**, *103*, 2421.
(73) Lovell, T.; Hino, F.; Han, W. G.; Noodleman, L. *Coord. Chem. Rev.* **2003**, *238*, 211.
(74) Eley, D. D.; Spivey, D. I. *Trans. Faraday Soc.* **1962**, *58*, 411.
(75) Eley, D. D.; Leslie, R. B. *Nature* **1963**, *197*, 898.
(76) Murphy, C. J.; Arkin, M. R.; Jenkins, Y.; Ghatlia, N. D.; Bossmann, S. H.; Turro, N. J.; Barton, J. K. *Science* **1993**, *262*, 1025.
(77) Priyadarshy, S.; Risser, S. M.; Beratan, D. N. *J. Phys. Chem.* **1996**, *100*, 17678.
(78) Beratan, D. N.; Priyadarshy, S.; Risser, S. M. *Chem. Biol.* **1997**, *4*, 3.
(79) (a) Debije, M. G.; Milano, M. T.; Bernhard, W. A. *Angew. Chem., Int. Ed.* **1999**, *38*, 2752. (b) Debije, M. G.; Bernhard, W. A. *J. Phys. Chem. B* **2000**, *104*, 7845.
(80) Boon, E. M.; Livingston, A. L.; Chmiel, N. H.; David, S. S.; Barton, J. K. *Proc. Natl. Acad. Sci. U.S.A.* **2003**, *100*, 12543.
(81) DeRosa, M. C.; Sancar, A.; Barton, J. K. *Proc. Natl. Acad. Sci. U.S.A.* **2005**, *102*, 10788.
(82) Boon, E. M.; Ceres, D. M.; Drummond, T. G.; Hill, M. G.; Barton, J. K. *Nat. Biotechnol.* **2000**, *18*, 1096.
(83) Porath, D.; Bezryadin, A.; de Vries, S.; Dekker, C. *Nature* **2000**, *403*, 635.
(84) Okamoto, A.; Tanaka, K.; Saito, I. *J. Am. Chem. Soc.* **2004**, *126*, 9458.
(85) Porath, D.; Cuniberti, G.; Di Felice, R. *Top. Curr. Chem.* **2004**, *237*, 183.
(86) Gorodetsky, A. A.; Buzzeo, M. C.; Barton, J. K. *Bioconjugate Chem.* **2008**, *19*, 2285.
(87) Diederichsen, U. *Angew. Chem., Int. Ed. Engl.* **1997**, *36*, 2317.
(88) Ratner, M. *Nature* **1999**, *397*, 480.
(89) Grinstaff, M. W. *Angew. Chem., Int. Ed.* **1999**, *38*, 3629.
(90) Hall, D. B.; Holmlin, R. E.; Barton, J. K. *Nature* **1996**, *382*, 731.
(91) Núñez, M. E.; Hall, D. B.; Barton, J. K. *Chem. Biol.* **1999**, *6*, 85.
(92) Henderson, P. T.; Jones, D.; Hampikian, G.; Kan, Y. Z.; Schuster, G. B. *Proc. Natl. Acad. Sci. U.S.A.* **1999**, *96*, 8353.
(93) Meggers, E.; Michel-Beyerle, M. E.; Giese, B. *J. Am. Chem. Soc.* **1998**, *120*, 12950.
(94) Wagenknecht, H.-A. *Angew. Chem., Int. Ed.* **2003**, *42*, 2454.
(95) Pascaly, M.; Yoo, J.; Barton, J. K. *J. Am. Chem. Soc.* **2002**, *124*, 9083.
(96) Boon, E. M.; Barton, J. K. *Curr. Opin. Struct. Biol.* **2002**, *12*, 320.
(97) Núñez, M. E.; Barton, J. K. *Curr. Opin. Chem. Biol.* **2000**, *4*, 199.
(98) Erkkila, K. E.; Odom, D. T.; Barton, J. K. *Chem. Rev.* **1999**, *99*, 2777.

(99) Meggers, E.; Kusch, D.; Spichty, M.; Wille, U.; Giese, B. *Angew. Chem., Int. Ed.* **1998**, *37*, 459.
(100) Giese, B. *Curr. Opin. Chem. Biol.* **2002**, *6*, 612.
(101) Giese, B. *Acc. Chem. Res.* **2000**, *33*, 631.
(102) Giese, B. *Annu. Rev. Biochem.* **2002**, *71*, 51.
(103) Bernhard, K.; Geimer, J.; Canle-Lopez, M.; Reynisson, J.; Beckert, D.; Gleiter, R.; Steenken, S. *Chem.—Eur. J.* **2001**, *7*, 4640.
(104) Shukla, L. I.; Adhikary, A.; Pazdro, R.; Becker, D.; Sevilla, M. D. *Nucleic Acids Res.* **2004**, *32*, 6565.
(105) Munk, B. H.; Burrows, C. J.; Schlegel, H. B. *Chem. Res. Toxicol.* **2007**, *20*, 432.
(106) Lewis, F. D.; Liu, X.; Miller, S. E.; Hayes, R. T.; Wasielewski, M. R. *J. Am. Chem. Soc.* **2002**, *124*, 11280.
(107) Lewis, F. D.; Liu, X.; Liu, J.; Miller, S. E.; Hayes, R. T.; Wasielewski, M. R. *Nature* **2000**, *406*, 51.
(108) Lewis, F. D.; Letsinger, R. L.; Wasielewski, M. R. *Acc. Chem. Res.* **2001**, *34*, 159.
(109) Lewis, F. D.; Liu, X.; Liu, J.; Hayes, R. T.; Wasielewski, M. R. *J. Am. Chem. Soc.* **2000**, *122*, 12037.
(110) Schuster, G. B. *Acc. Chem. Res.* **2000**, *33*, 253.
(111) Henderson, P. T.; Jones, D.; Hampikian, G.; Kan, Y.; Schuster, G. B. *Proc. Natl. Acad. Sci. U.S.A.* **1999**, *96*, 8353.
(112) Ly, D.; Kan, Y.; Armitage, B.; Schuster, G. B. *J. Am. Chem. Soc.* **1996**, *118*, 8747.
(113) Saito, I.; Nakamura, T.; Nakatani, K.; Yoshioka, Y.; Yamaguchi, K.; Sugiyama, H. *J. Am. Chem. Soc.* **1998**, *120*, 12686.
(114) Sugiyama, H.; Saito, I. *J. Am. Chem. Soc.* **1996**, *118*, 7063.
(115) Prat, F.; Houk, K. N.; Foote, C. S. *J. Am. Chem. Soc.* **1998**, *120*, 845.
(116) Lewis, F. D.; Liu, X.; Liu, J.; Hayes, R. T.; Wasielewski, M. R. *J. Am. Chem. Soc.* **2000**, *122*, 12037.
(117) Conwell, E. M.; Basko, D. M. *J. Am. Chem. Soc.* **2001**, *123*, 11441.
(118) Berlin, Y. A.; Burin, A. L.; Ratner, M. A. *J. Am. Chem. Soc.* **2001**, *123*, 260.
(119) Adhikary, A.; Khanduri, D.; Sevilla, M. D. *J. Am. Chem. Soc.* **2009**, *131*, 8614.
(120) Anderson, R. F.; Wright, G. A. *Phys. Chem. Chem. Phys.* **1999**, *1*, 4827.
(121) Anderson, R. F.; Patel, K. B. *J. Chem. Soc., Faraday Trans.* **1991**, *87*, 3739.
(122) Messer, A.; Carpenter, K.; Forzley, K.; Buchanan, J.; Yang, S.; Razskazovskii, Y.; Cai, Z.; Sevilla, M. D. *J. Phys. Chem. B* **2000**, *104*, 1128.
(123) Cai, Z.; Sevilla, M. D. *Top. Curr. Chem.* **2004**, *237*, 103.
(124) Schwögler, A.; Burgdorf, L. T.; Carell, T. *Angew. Chem., Int. Ed.* **2000**, *39*, 3918.
(125) Behrens, C.; Burgdorf, L. T.; Schwögler, A.; Carell, T. *Angew. Chem., Int. Ed.* **2002**, *41*, 1763.
(126) (a) Lewis, F. D.; Liu, X.; Wu, Y.; Miller, S. E.; Wasielewski, M. R.; Letsinger, R. L.; Sanishvili, R.; Joachimiak, A.; Tereshko, V.; Egli, M. *J. Am. Chem. Soc.* **1999**, *121*, 9905. (b) Lewis, F. D.; Liu, X.; Miller, S. E.; Hayes, R. T.; Wasielewski, M. R. *J. Am. Chem. Soc.* **2002**, *124*, 11280.
(127) (a) Giese, B.; Carl, B.; Carl, T.; Carell, T.; Behrens, C.; Hennecke, U.; Schiemann, O.; Feresin, E. *Angew. Chem., Int. Ed.* **2004**, *43*, 1848. (b) Schiemann, O.; Feresin, E.; Carl, T.; Giese, B. *ChemPhysChem* **2004**, *5*, 270.
(128) Jortner, J.; Bixon, M.; Langenbacher, T.; Michel-Beyerle, M. E. *Proc. Natl. Acad. Sci. U.S.A.* **1998**, *95*, 12759.
(129) Marcus, R. A.; Sutin, N. *Biochim. Biophys. Acta* **1985**, *811*, 265.
(130) Bixon, M.; Jortner, J. *Chem. Phys.* **2002**, *281*, 393.
(131) Grozema, F. C.; Berlin, Y. A.; Siebbeles, L. D. A. *J. Am. Chem. Soc.* **2000**, *122*, 10903.
(132) Purugganan, M. D.; Kumar, C. V.; Turro, N. J.; Barton, J. K. *Science* **1988**, *241*, 1645.
(133) Kelley, S. O.; Barton, J. K. *Science* **1999**, *283*, 375.
(134) Turro, N. J.; Barton, J. K. *J. Biol. Inorg. Chem.* **1998**, *3*, 201.
(135) Giese, B.; Amaudrut, J.; Kohler, A.-K.; Spormann, M.; Wessely, S. *Nature* **2001**, *412*, 318.
(136) Meggers, E.; Kusch, D.; Spichty, M.; Wille, U.; Giesse, B. *Angew. Chem., Int. Ed.* **1998**, *37*, 460.
(137) Lewis, F. D.; Wu, T.; Zhang, Y.; Letsinger, R. L.; Greenfield, S. R.; Wasielewski, M. R. *Science* **1997**, *277*, 673.
(138) Fukui, K.; Tanaka, K. *Angew. Chem., Int. Ed.* **1998**, *37*, 158.
(139) Grozema, F. C.; Berlin, Y. A.; Siebbeles, L. D. A. *Int. J. Quantum Chem.* **1999**, *75*, 1009.
(140) Olofsson, J.; Larsson, S. *J. Phys. Chem. B* **2001**, *105*, 10398.
(141) Conwell, E. M.; McLaughlin, P. M.; Bloch, S. M. *J. Phys. Chem. B* **2008**, *112*, 2268.
(142) Conwell, E. M. *Proc. Natl. Acad. Sci. U.S.A.* **2005**, *102*, 8795.
(143) Conwell, E. M.; Bloch, S. M. *J. Phys. Chem. B* **2006**, *110*, 5801.
(144) Conwell, E. M.; Bloch, S. M.; McLaughlin, P. M.; Basko, D. M. *J. Am. Chem. Soc.* **2007**, *129*, 9175.
(145) Kanvah, S.; Joseph, J.; Schuster, G. B.; Barnett, R. N.; Cleveland, C. L.; Landman, U. *Acc. Chem. Res.* **2010**, *43*, 280.
(146) Barnett, R. N.; Cleveland, C. L.; Joy, A.; Landman, U.; Schuster, G. B. *Science* **2001**, *294*, 567.
(147) Genereux, J. C.; Barton, J. K. *Chem. Rev.* **2010**, *110*, 1642.
(148) Prunkl, C.; Berndl, S.; Wanninger-Weiβ, C.; Barbaric, J.; Wagenknecht, H.-A. *Phys. Chem. Chem. Phys.* **2010**, *12*, 32.
(149) Wagenknecht, H. A., Ed. *Charge Transfer in DNA*; Wiley-VCH: Weinheim, Germany, 2005.
(150) Schuster, G. B., Ed. *Long-Range Charge Transfer in DNA, I and II*; Springer: New York, 2004; Vols. *236* and *237*.
(151) Reece, S. Y.; Nocera, D. G. *Annu. Rev. Biochem.* **2009**, *78*, 673.
(152) Cukier, R. I. *J. Phys. Chem. B* **2002**, *106*, 1746.
(153) Cukier, R. I. *J. Phys. Chem.* **1994**, *98*, 2377.
(154) Cukier, R. I. *J. Phys. Chem.* **1995**, *99*, 16101.
(155) Zhao, X. G.; Cukier, R. I. *J. Phys. Chem.* **1995**, *99*, 945.
(156) Cukier, R. I. *J. Phys. Chem.* **1996**, *100*, 15428.
(157) Cukier, R. I. *Biochim. Biophys. Acta* **2004**, *1655*, 37.
(158) Soudackov, A.; Hammes-Schiffer, S. *J. Chem. Phys.* **1999**, *111*, 4672.
(159) Soudackov, A.; Hammes-Schiffer, S. *J. Chem. Phys.* **2000**, *113*, 2385.
(160) Soudackov, A.; Hatcher, E.; Hammes-Schiffer, S. *J. Chem. Phys.* **2005**, *122*, 014505.
(161) Ludlow, M. K.; Skone, J. H.; Hammes-Schiffer, S. *J. Phys. Chem. B* **2008**, *112*, 336.
(162) Hammes-Schiffer, S.; Soudackov, A. *J. Phys. Chem. B* **2008**, *112*, 14108.
(163) Edwards, S. J.; Soudackov, A. V.; Hammes-Schiffer, S. *J. Phys. Chem. B* **2009**, *113*, 14545.
(164) Mayer, J. M. *Annu. Rev. Phys. Chem.* **2004**, *55*, 363.
(165) Costentin, C.; Robert, M.; Saveant, J.-M. *J. Am. Chem. Soc.* **2006**, *128*, 4552.
(166) Georgievskii, Y.; Stuchebrukhov, A. A. *J. Chem. Phys.* **2000**, *113*, 10438.
(167) Turró, C.; Chang, C. K.; Leroi, G. E.; Cukier, R. I.; Nocera, D. G. *J. Am. Chem. Soc.* **1992**, *114*, 4013.
(168) Skone, J. H.; Soudackov, A. V.; Hammes-Schiffer, S. *J. Am. Chem. Soc.* **2006**, *128*, 16655.
(169) Mayer, J. M.; Hrovat, D. A.; Thomas, J. L.; Borden, W. T. *J. Am. Chem. Soc.* **2002**, *124*, 11142.
(170) Taylor, J.; Eliezer, I.; Sevilla, M. D. *J. Phys. Chem. B* **2001**, *105*, 1614.
(171) Carra, C.; Iordanova, N.; Hammes-Schiffer, S. *J. Phys. Chem. B* **2002**, *106*, 8415.
(172) Candeias, L. P.; Steenken, S. *J. Am. Chem. Soc.* **1989**, *111*, 1094.
(173) Candeias, L. P.; Steenken, S. *J. Am. Chem. Soc.* **1992**, *114*, 699.
(174) Shafirovich, V.; Dourandin, A.; Luneva, N. P.; Geacintov, N. E. *J. Phys. Chem. B* **2000**, *104*, 137.
(175) Kuzmin, V. A.; Dourandin, A.; Shafirovich, V.; Geacintov, N. E. *Phys. Chem. Chem. Phys.* **2000**, *2*, 1531.
(176) Shafirovich, V.; Dourandin, A.; Geacintov, N. E. *J. Phys. Chem. B* **2001**, *105*, 8431.
(177) Shafirovich, V.; Dourandin, A.; Huang, W. D.; Luneva, N. P.; Geacintov, N. E. *Phys. Chem. Chem. Phys.* **2000**, *2*, 4399.
(178) Shafirovich, V.; Cadet, J.; Gasparutto, D.; Dourandin, A.; Huang, W. D.; Geacintov, N. E. *J. Phys. Chem. B* **2001**, *105*, 586.
(179) Shafirovich, V. Ya.; Courtney, S. H.; Ya, N.; Geacintov, N. E. *J. Am. Chem. Soc.* **1995**, *117*, 4920.
(180) Weatherly, S. C.; Yang, I. V.; Armistead, P. A.; Thorp, H. H. *J. Phys. Chem. B* **2003**, *107*, 372.
(181) Weatherly, S. C.; Yang, I. V.; Thorp, H. H. *J. Am. Chem. Soc.* **2001**, *123*, 1236.
(182) Chatgilialoglu, C.; Caminal, C.; Guerra, M.; Mulazzani, Q. G. *Angew. Chem., Int. Ed.* **2005**, *44*, 6030.
(183) Mundy, C. J.; Colvin, M. E.; Quong, A. A. *J. Phys. Chem. A* **2002**, *106*, 10063.
(184) Adhikary, A.; Kumar, A.; Becker, D.; Sevilla, M. D. *J. Phys. Chem. B* **2006**, *110*, 24171, and references therein.
(185) Ortmans, I.; Elias, B.; Kelly, J. M.; Moucheron, C.; Kirsch-DeMesmaeker, A. *Dalton Trans.* **2004**, 668.
(186) Elias, B.; Creely, C.; Doorley, G. W.; Feeney, M. M.; Moucheron, C.; Kirsch-DeMesmaeker, A.; Dyer, J.; Grills, D. C.; George, M. W.; Matousek, P.; Parker, A. W.; Towrie, M.; Kelly, J. M. *Chem.—Eur. J.* **2008**, *14*, 369.
(187) Kobayashi, K.; Tagawa, S. *J. Am. Chem. Soc.* **2003**, *125*, 10213.
(188) Kobayashi, K.; Yamagami, R.; Tagawa, S. *J. Phys. Chem. B* **2008**, *112*, 10752.
(189) Giese, B.; Wessely, S. *Chem. Commun.* **2001**, 2108.
(190) Takada, T.; Kawai, K.; Fujitsuka, M.; Majima, T. *Chem.—Eur. J.* **2005**, *11*, 3835.
(191) Kawai, K.; Osakada, Y.; Majima, T. *ChemPhysChem* **2009**, *10*, 1766.
(192) Stemp, E. D. A.; Arkin, M.; Barton, J. K. *J. Am. Chem. Soc.* **1997**, *119*, 2921.

(193) Schiemann, O.; Turro, N. J.; Barton, J. K. *J. Phys. Chem. B* **2000**, *104*, 7214.
(194) Anderson, R. F.; Shinde, S. S.; Maroz, A. *J. Am. Chem. Soc.* **2006**, *128*, 15966.
(195) Gervasio, F. L.; Boero, M.; Parrinello, M. *Angew. Chem., Int. Ed.* **2006**, *45*, 5606.
(196) Colson, A. O.; Besler, B.; Sevilla, M. D. *J. Phys. Chem.* **1992**, *96*, 9787.
(197) Hutter, M.; Clark, T. *J. Am. Chem. Soc.* **1996**, *118*, 7574.
(198) Bertran, J.; Oliva, A.; Rodriguez-Santiago, L.; Sodupe, M. *J. Am. Chem. Soc.* **1998**, *120*, 8159.
(199) Li, X. F.; Cai, Z. L.; Sevilla, M. D. *J. Phys. Chem. B* **2001**, *105*, 10115.
(200) Kumar, A.; Sevilla, M. D. *J. Phys. Chem. B.* **2009**, *113*, 11359.
(201) Sobolewski, A. L.; Domcke, W. *Phys. Chem. Chem. Phys.* **2004**, *6*, 2763.
(202) Sobolewski, A. L.; Domcke, W.; Hattig, C. *Proc. Natl. Acad. Sci. U.S.A.* **2005**, *102*, 17903.
(203) Abu-Riziq, A.; Grace, L.; Nir, E.; Kabelac, M.; Hobza, P.; de Vries, M. S. *Proc. Natl. Acad. Sci. U.S.A.* **2005**, *102*, 20.
(204) Schwalb, N. K.; Temps, F. *J. Am. Chem. Soc.* **2007**, *129*, 9272.
(205) Groenhof, G.; Schäfer, L. V.; Boggio-Pasqua, M.; Goette, M.; Grubmüller, H.; Robb, M. A. *J. Am. Chem. Soc.* **2007**, *129*, 6812.
(206) Crespo-Hernández, C. E.; de La Harpe, K.; Kohler, B. *J. Am. Chem. Soc.* **2008**, *130*, 10844.
(207) de La Harpe, K.; Crespo-Hernández, C. E.; Kohler, B. *J. Am. Chem. Soc.* **2009**, *131*, 17557.
(208) Milligan, J. R.; Aguilera, J. A.; Hoang, O.; Ly, A.; Tran, N. Q.; Ward, J. F. *J. Am. Chem. Soc.* **2004**, *126*, 1682.
(209) Ly, A.; Tran, N. Q.; Ward, J. F.; Milligan, J. R. *Biochemistry* **2004**, *43*, 9098.
(210) Ly, A.; Tran, N. Q.; Sullivan, K.; Bandong, S. L.; Milligan, J. R. *Org. Biomol. Chem.* **2005**, *3*, 917.
(211) Llano, J.; Eriksson, L. A. *Phys. Chem. Chem. Phys.* **2004**, *6*, 4707.
(212) Jena, N. R.; Mishra, P. C.; Suhai, S. *J. Phys. Chem. B* **2009**, *113*, 5633.
(213) Sevilla, M. D.; Paemel, C. V.; Nichols, C. *J. Phys. Chem.* **1972**, *76*, 3571.
(214) Sevilla, M. D.; Paemel, C. V.; Nichols, C. *J. Phys. Chem.* **1972**, *76*, 3577.
(215) Sevilla, M. D. *J. Phys. Chem.* **1971**, *75*, 626.
(216) Geimer, J.; Hildenbrand, K.; Naumov, S.; Beckert, D. *Phys. Chem. Chem. Phys.* **2000**, *2*, 4199.
(217) Krivokapic′, A.; Herak, J. N.; Sagstuen, E. *J. Phys. Chem. A* **2008**, *112*, 3597.
(218) Nelson, W. H.; Sagstuen, E.; Hole, E. O.; Close, D. M. *Radiat. Res.* **1998**, *149*, 75.
(219) Shi, Y.; Huang, C.; Wang, W.; Kang, J.; Yao, S.; Lin, N.; Zheng, R. *Radiat. Phys. Chem.* **2000**, *58*, 253.
(220) Adhikary, A.; Kumar, A.; Khanduri, D.; Sevilla, M. D. *J. Am. Chem. Soc.* **2008**, *130*, 10282.
(221) Perun, S.; Sobolewski, A. L.; Domcke, W. *J. Phys. Chem. A* **2006**, *110*, 9031.
(222) Adhikary, A.; Collins, S.; Koppen, J.; Becker, D.; Sevilla, M. D. *Nucleic Acids Res.* **2006**, *34*, 1501.
(223) Adhikary, A.; Malkhasian, A. Y. S.; Collins, S.; Koppen, J.; Becker, D.; Sevilla, M. D. *Nucleic Acids Res.* **2005**, *33*, 5553.
(224) Adhikary, A.; Collins, S.; Khanduri, D.; Sevilla, M. D. *J. Phys. Chem. B* **2007**, *111*, 7415.
(225) Khanduri, D.; Collins, S.; Kumar, A.; Adhikary, A.; Sevilla, M. D. *J. Phys. Chem. B* **2008**, *112*, 2168.
(226) Adhikary, A.; Khanduri, D.; Kumar, A.; Sevilla, M. D. *J. Phys. Chem. B* **2008**, *112*, 15844.
(227) Becker, D.; Razskazovskii, Y.; Callaghan, M. U.; Sevilla, M. D. *Radiat. Res.* **1996**, *146*, 361.
(228) Kumar, A.; Sevilla, M. D. *J. Phys. Chem. B* **2009**, *113*, 13374.
(229) Hammond, G. S. *J. Am. Chem. Soc.* **1955**, *77*, 334.
(230) Aflatooni, K.; Gallup, G. A.; Burrow, P. D. *J. Phys. Chem. A* **1998**, *102*, 6205.
(231) Rak, J.; Mazurkiewicz, K.; Kobyłecka, M.; Storoniak, P.; Harańczyk, M.; Dąbkowska, I.; Bachorz, R. A.; Gutowski, M.; Radisic, V.; Stokes, S. T.; Eustis, S. N.; Wang, D.; Li, X.; Ko, Y. J.; Bowen, K. H. In *Radiation Induced Molecular Phenomena in Nucleic Acids*; Shukla, M. K., Leszczynski, J., Eds.; Challenges and Advances in Computational Chemistry and Physics, Vol. 5; Leszczynski, J., Ed.; Springer Science + Business Media B.V.: Dordrecht, The Netherlands, 2008; pp 619−667.
(232) Nelson, W. H.; Hole, E. O.; Sagstuen, E.; Close, D. M. *Int. J. Radiat. Biol.* **1988**, *54*, 963.
(233) (a) Jayatilaka, N.; Nelson, W. H. *J. Phys. Chem. B* **2008**, *112*, 16908. (b) Nelson, W. H.; Sagstuen, E.; Hole, E. O.; Close, D. M. *Radiat. Res.* **1992**, *131*, 10.
(234) Bernhard, W. A. *Adv. Radiat. Biol.* **1981**, *9*, 199.
(235) Wang, W.; Sevilla, M. D. *Radiat. Res.* **1994**, *138*, 9.
(236) Candeias, L. P.; Wolf, P.; O'Neill, P.; Steenken, S. *J. Phys. Chem.* **1992**, *96*, 10302.
(237) Harańczyk, M.; Gutowski, M.; Li, X.; Bowen, K. H. *J. Phys. Chem. B* **2007**, *111*, 14073.
(238) Harańczyk, M.; Gutowski, M. *Angew. Chem., Int. Ed.* **2005**, *44*, 6585.
(239) Harańczyk, M.; Gutowski, M. *J. Am. Chem. Soc.* **2005**, *127*, 699.
(240) Chatgilialoglu, C.; D'Angelantonio, M.; Kaloudis, P.; Mulazzani, Q. G.; Guerra, M. *J. Phys. Chem. Lett.* **2010**, *1*, 174.
(241) Yamagami, R.; Kobayashi, K.; Tagawa, S. *J. Am. Chem. Soc.* **2008**, *130*, 14772.
(242) Szyperska, A.; Rak, J.; Leszczynski, J.; Li, X.; Ko, Y. J.; Wang, H.; Bowen, K. H. *J. Am. Chem. Soc.* **2009**, *131*, 2663.
(243) Colson, A.-O.; Besler, B.; Sevilla, M. D. *J. Phys. Chem.* **1992**, *96*, 9181.
(244) Gu, J.; Xie, Y.; Schaefer, H. F. *J. Chem. Phys.* **2007**, *127*, 155107.
(245) Chen, H.-Y.; Kao, C.-L.; Hsu, S. C. N. *J. Am. Chem. Soc.* **2009**, *131*, 15930.
(246) Chen, H.-Y.; Hsu, S. C. N.; Kao, C.-L. *Phys. Chem. Chem. Phys.* **2010**, *12*, 1253.
(247) Sagstuen, E.; Hole, E. O.; Nelson, W. H.; Close, D. M. *J. Phys. Chem.* **1989**, *93*, 5974.
(248) (a) Hole, E. O.; Sagstuen, E.; Nelson, W. H.; Close, D. M. *J. Phys. Chem.* **1991**, *95*, 1494. (b) Sagstuen, E.; Hole, E. O.; Nelson, W. H.; Close, D. M. *J. Phys. Chem.* **1992**, *96*, 8269.
(249) Barnes, J.; Bernhard, W. A.; Mercer, K. R. *Radiat. Res.* **1991**, *126*, 104.
(250) Hissung, A.; Von Sonntag, C. *Int. J. Radiat. Biol.* **1979**, *35*, 449.
(251) Schuchmann, H.-P.; Von Sonntag, C. *Int. J. Radiat. Biol.* **1986**, *49*, 1.
(252) Mroczka, N. E.; Mercer, K. R.; Bernhard, W. A. *Radiat. Res.* **1997**, *147*, 560.
(253) Raytchev, M.; Mayer, E.; Amann, N.; Wagenknecht, H.-A.; Fiebig, T. *ChemPhysChem* **2004**, *5*, 706.
(254) Netzel, T. L.; Zhao, M.; Nafisi, K.; Headrick, J.; Sigman, M. S.; Eaton, B. E. *J. Am. Chem. Soc.* **1995**, *117*, 9119.
(255) Cai, Z.; Li, X.; Sevilla, M. D. *J. Phys. Chem. B* **2002**, *106*, 2755.
(256) Harańczyk, M.; Rak, J.; Gutowski, M. *J. Phys. Chem. A* **2005**, *109*, 11495.
(257) Harańczyk, M.; Gutowski, M.; Warshel, A. *Phys. Chem. Chem. Phys.* **2008**, *10*, 4442.
(258) Harańczyk, M.; Rak, J.; Gutowski, M.; Radisic, D.; Stokes, S. T.; Bowen, K. H. *J. Phys. Chem. B* **2005**, *109*, 13383.
(259) Visscher, K. J.; De Haas, M. P.; Loman, H.; Vojnovic, B.; Warman, J. M. *Int. J. Radiat. Biol.* **1987**, *52*, 745.
(260) Candeias, L. P.; Steenken, S. *J. Phys. Chem.* **1992**, *96*, 937.
(261) Stokes, S. T.; Grubisic, A.; Li, X.; Ko, Y. J.; Bowen, K. H. *J. Chem. Phys.* **2008**, *128*, 044314.
(262) Li, X.; Bowen, K. H.; Harańczyk, M.; Bachorz, R. A.; Mazurkiewicz, K.; Rak, J.; Gutowski, M. *J. Chem. Phys.* **2007**, *127*, 174309.
(263) Mazurkiewicz, K.; Harańczyk, M.; Gutowski, M.; Rak, J.; Radisic, D.; Eustis, S. N.; Wang, D.; Bowen, K. H. *J. Am. Chem. Soc.* **2007**, *129*, 1216.
(264) Mazurkiewicz, K.; Harańczyk, M.; Storoniak, P.; Gutowski, M.; Rak, J.; Radisic, D.; Eustis, S. N.; Wang, D.; Bowen, K. H. *Chem. Phys.* **2007**, *342*, 215.
(265) Radisic, D.; Bowen, K. H.; Dąbkowska, I.; Storoniak, P.; Rak, J.; Gutowski, M. *J. Am. Chem. Soc.* **2005**, *127*, 6443.
(266) Martin, F.; Burrow, P. D.; Cai, Z.; Cloutier, P.; Hunting, D.; Sanche, L. *Phys. Rev. Lett.* **2004**, *93*, 068101.
(267) Panajotovic, R.; Martin, F.; Cloutier, P. C.; Hunting, D.; Sanche, L. *Radiat. Res.* **2006**, *165*, 452.
(268) Li, X.; Sevilla, M. D.; Sanche, L. *J. Am. Chem. Soc.* **2003**, *125*, 13668.
(269) Simons, J. *Acc. Chem. Res.* **2006**, *39*, 772.
(270) Bao, X.; Wang, J.; Gu, J.; Leszczynski, J. *Proc. Natl. Acad. Sci. U.S.A.* **2006**, *103*, 5658.
(271) Kumar, A.; Sevilla, M. D. *J. Phys. Chem. B* **2007**, *111*, 5464.
(272) Kumar, A.; Sevilla, M. D. *J. Am. Chem. Soc.* **2008**, *130*, 2130.
(273) Kumar, A.; Sevilla, M. D. *ChemPhysChem* **2009**, *10*, 1426.
(274) Dąbkowska, I.; Rak, J.; Gutowski, M. *Eur. Phys. J. D* **2005**, *35*, 429.
(275) Gu, J.; Wang, J.; Rak, J.; Leszczynski, J. *Angew. Chem., Int. Ed.* **2007**, *46*, 3479.

CR100023G